Journal notes on:

Introduction to topological superconductivity

by Francisco Lobo

CONTENTS

ACKNOWLEDGMENTS

My personal website is at https://franciscolobo1880.github.io/.

As supplementary material, there is a GitHub repository at https://github.com/franciscolobo1880/topoSC where you can check the code that generate the figures of the various models. This is done in *Julia* using the *Quantica.jl* package by Pablo San-Jose, my PhD advisor. Check *Quantica.jl*'s repository and it's tutorial at https://github.com/pablosanjose/Quantica.jl.

I thank Pablo San-Jose and Elsa Prada for their tutoring. I thank César Robles, Carlos Paya and Tiago Antão for their help and useful discussions.

PREFACE

This introduction is recycled from a draft I had. It does not fit entirely here but serves as a somewhat decent placeholder. Ever since Kamerlingh Onnes discovered the "zero resistance state" of metals at very low temperatures in 1911, the superconducting state of matter has fascinated physicists. Notably, Bardeen–Cooper–Schrieffer's (BCS) theory of superconductivity was a watershed in modern condensed matter physics. It's key feature is pair condensation, the macroscopic occupation of a bound state of fermion pairs. The binding of fermions into Cooper pairs typically leads to an energy gap in the fermionic excitation spectrum, while condensation of Cooper pairs leads to the breaking of global $U(1)$ gauge symmetry. This symmetry breaking is linked to the spontaneously choosing of an overall phase φ of the macroscopic wavefunction below the transition temperature T_c (akin to how a ferromagnet spontaneously picks a magnetization direction) and it's generator is the particle number, being related to the fact that φ and N are canonical conjugate (well, technically only for larger values of N but this is often the case). In BCS superconductivity considerations, φ is precisely the (conjugate of the) number of Cooper pairs formed. Furthermore, the symmetry breaking of $U(1)$ implies that the fermionic excitations are no longer charge eigenstates, but each is a coherent superposition of a normal-state particle and hole, e.g. $\gamma_{\mathbf{k}\sigma} = u_{\mathbf{k}}\psi_{\mathbf{k}\sigma} + v^*_{\mathbf{k}}\psi^\dagger_{-\mathbf{k}\bar{\sigma}}$, with $\psi/\psi^\dagger$ the electronic field operators and where u and v are the particle and hole amplitudes (defined by momentum $\mathbf{k}$ and spin σ [$\bar{\sigma}$ being the flipped spin]) defining the so called Bogoliubov quasi-particles (or Bogoliubons). Charge conservation is then maintained by an additional channel for charge transport via the coherent motion of the pair condensate. One can then construct the ground state of the superconductor $|\emptyset\rangle$ (also denoted as $|\mathrm{GS}\rangle$ or $|\mathrm{BCS}\rangle$) from the condition that it contain no Bogoliubons, $\gamma\,|\emptyset\rangle = 0$, wielding a superposition of states with different number of Cooper pairs $|\emptyset\rangle = \prod_{\mathbf{k}}(u_{\mathbf{k}} - v^*_{\mathbf{k}}\psi^\dagger_{\mathbf{k}\sigma}\psi^\dagger_{-\mathbf{k}\bar{\sigma}})\,|0\rangle$, with $|0\rangle$ the state containing no electrons.

Expanding beyond BCS, we can distinguish other types of superconductivity by the characteristics of the pair condensation. In BCS superconductors (SCs), the electrons are being Cooper paired with opposite spins, forming a $S = 0$ spin-singlet state, but it possible to Cooper pair electrons with parallel spins forming three possible $S = 1$ spin-triplet states without violating Pauli principle. Concerning with the orbital component we can also distinguish between different angular momentums $\ell = 0(s), 1(p), 2(d), 3(f)$ and so on. As a first order approximation, one can match the orbital component to the shapes of spherical harmonics, although, of course, with the caveat that the crystal lattice and Fermiology can make the situation more complex in real materials. Because Fermions obey antisymmetric exchange (switching two electrons corresponds to a sign change), if the spin part of the wavefunction is antisymmetric, as is the case for the singlet case, then the orbital part has to be even, $\ell = 0, 2, ...$ Of course, for the same reason, the triplet case must have instead odd orbital part, $\ell = 1, 3, ...$

This different types of SCs can also be discussed in terms of a quantity Δ known as the order parameter. For example, in Ginzburh-Landau (GL) theory Δ is emblematic of a phenomenological "wavefunction" for the superconducting fluid while in BCS theory it has to do with the "wavefunction" of the Cooper pairs, being named interchangeably as pairing potential. Spatial variations of the pairing potential lead to modifications of the coherence amplitudes u and v mentioned above, particularly to a novel scattering dubbed Andreev scattering (or branch conversion scattering).

For instance, such is the case of states trapped at weak links between SCs or at a semiconductor-superconductor (SM-SC) interface; when an electron (within the SM) has an energy below the SC gap (i.e forbidden to simply propagate into the SC) hits the SM-SC interface (assumed to be highly transparent, e.g with no oxide or tunnel layer, the incident electron forms a Cooper pair in the superconductor with the retro-reflection of a hole of opposite spin and velocity but equal momentum to the incident electron, as seen the figure below. Of course, through time-reversal symmetry, the process will also work with an incident hole. If the interface is highly transparent, below the SC gap such Andreev process dominates with high probability, whereas in the opposite limit the electron is specularly reflected. In regions of strong spatial variations, multiple Andreev reflection leads to the

formation of sub-gap states, Andreev bound states (ABS). The presence of such bound states has important consequences for transport since it implies that a normal metal can carry a dissipationless supercurrent $I_A(\varphi)$ between two SCs over arbitrarily long lengths, provided that transport is coherent. This is the celebrated DC Josephson effect.

With the advent of topological (TP) materials, the existence of new states of matter known collectively as topological superconducting (TP SC) phases have been predicted, arising particularly in p-wave SCs. Topological SC phases are characterized by the emergence of a rather special type of subgap bound state occurring at topological defects such as vortices, boundaries or domain walls. Importantly, such bound states occur precisely at zero energy, and exhibit electron and hole character with exactly equal probability. The second quantization operators describing these states are thus self-conjugate $\gamma = \gamma^\dagger$, meaning that they are is its own antiparticle, unlike Dirac fermions, and will effectively behave as fractionalized objects, known as anyons, obeying non-Abelian anyonic statistics rather than Fermi or Bose statistics. They are in this sense a condensed matter realization of the celebrated states known as Majorana fermions (MFs). As opposed to standard Andreev bound states, which can be pushed out of the gap by continuous deformations of the Hamiltonian, Majorana bound states (MBSs) candiscossionsnot be removed from zero energy by any local perturbation or local noise that does not close the gap. This robust zero-energy pinning is a consequence of the bulk-boundary correspondence principle of band topology, which predicts that at the boundaries between materials with different topological indices, edge states must appear that are protected against perturbations by the topology of the bulk.

I. OVERVIEW OF SUPERCONDUCTIVITY FOUNDATIONAL THEORIES

As a precursor to topological superconductivity theory, we make a brief recap of the main superconductivity theories. Our intentions is not to make a complete mathematical description of said theories but act more as a memory refreshment of the core ideas and concepts. Also, since this section will serve more as consultation, we highlight the famous, useful, equations, be omitting any derivations (although somewhat explaining it in text so one can follow). I will try to keep a linear storytelling of the various theories with some exception of qualitatively nodding to context further ahead in the text to strengthen intuition.

A. London theory

The first theoretical explanation for the occurrence of superconductivity in metallic superconductors was proposed by the London brothers, Fritz London and Heinz London, in 1935. They began with the premise that if electrons in a superconductor do not encounter resistance, they will continue to accelerate under the influence of an applied electric field. Under this notion, they formulated the London equations, which serve as constitutive relations for a superconductor, describing the relationship between its superconducting current and the surrounding electromagnetic fields. While Ohm's law represents the simplest constitutive relation for an ordinary conductor, the London equations provide the most fundamental and meaningful description of superconducting phenomena.

London equations

Let us then start from the base concept of electrons accelerating with no resistance under the influence of an applied electric field $\mathbf{E}$. The equation of motion of these electrons in the superconducting state will then read $m\,(d\mathbf{v}_s/dt) = -e\mathbf{E}$ with m, $\mathbf{v}_s$, e and n_s their mass, velocity, charge and density respectively. On the other hand, the superconducting current density is given by $\mathbf{J}_s = -en_s\mathbf{v}_s$. Differentiating it with respect to time and substituting $d\mathbf{v}_s/dt$ yields the first London equation

$$\frac{d\mathbf{J}_s}{dt} = \frac{n_s e^2}{m}\mathbf{E} \tag{1}$$

Furthermore, taking the curl on both sides, making use of Faraday's law $\boldsymbol{\nabla}\times\mathbf{E} = -\partial_t\mathbf{B}$, and integrating both sides of the equation on obtains the second London equation

$$\boldsymbol{\nabla}\times\mathbf{J}_s = -\frac{n_s e^2}{m}\mathbf{B} \tag{2}$$

where the constant of integration is set zero to account for the fact that there is no resistivity in superconductors.

1. *London penetration depth and Meissner effect*

Consider Ampere's law $\boldsymbol{\nabla}\times\mathbf{B} = -\mu_0\mathbf{J}$, with μ_0 the vacuum magnetic permeability, which relates the magnetic field along a closed path to the total current following through any surface bounded by the path. If one takes its curl from both sides and makes use the no magnetic monopole law $\boldsymbol{\nabla}\cdot\mathbf{B} = 0$ one obtains $\boldsymbol{\nabla}^2\mathbf{B} = -\mu_0\boldsymbol{\nabla}\times\mathbf{J}$. Substituting the curl of the generic current $\mathbf{J}$ for our superconducting current $\mathbf{J}_s$ as given by London's 2nd equation one obtains the equation that describes the Meissner effect, reading

$$\boldsymbol{\nabla}^2\mathbf{B} = \left(\mu_0\frac{n_s e^2}{m}\right)\mathbf{B} \equiv \frac{1}{\lambda_0^2}\mathbf{B} \tag{3}$$

where λ_0^2 has dimension of length and is known as London's penetration depth. This equation tells us that that the magnetic field is exponentially suppressed as it penetrates inward a bulk superconductor. For example, see that a magnetic field $\mathbf{B} = B\hat{\mathbf{z}}$ that penetrates a superconductor within the semi-infinite plane $x\mathcal{O}z$ is damped as $\mathbf{B}(x) = B_0 \exp(-x/\lambda_0)\hat{\mathbf{z}}$ while inside the superconductor.

This exclusion of magnetic field is a manifestation of the superdiamagnetism emerged during the phase transition from conductor to superconductor, for example by reducing the temperature below critical temperature. In the presence of a weak external magnetic field—one that is below the critical threshold for the breakdown of superconductivity—a superconductor nearly completely expels the magnetic flux by generating electric currents in a thin layer near its surface. Specifically, the magnetic field induces a magnetization within the London penetration depth, which in turn establishes screening currents. These currents serve to protect the superconductor's internal bulk from the external field. Moreover, because the flux expulsion remains invariant over time, the so-called persistent (or screening) currents sustaining this effect do not decay.

See that this penetration depth is inversely proportional to the square root of the electron density in the superconductive state n_s, which in turn should depend on temperature. Concretely, one expects that as the temperature rises, n_s decreases and, consequently, the extent of flux penetration increases. At some critical temperature T_c, n_s drops to zero, allowing the magnetic field to fully penetrate the material and causing the superconductor to revert to its normal state. The London brothers did not find exactly what this temperature dependence law should look and mostly miscalculated λ_0 of different materials just because n_s could not be merely treated as a free electron density as it is done on metals; rather, the electrons in these superconductive phase were latter found to interact coherently. The actual temperature-dependent London penetration depth will be described in the next section.

2. London coherence length

In addition to the London penetration depth λ_L, there is another th fundamental length scale that governs superconducting behavior. Together, these two length scales play a crucial role in defining the properties of a superconductor.

While λ_L characterizes the extent to which an external magnetic field can penetrate a superconductor, ξ defines the spatial region over which the superconducting electron density remains relatively uniform, preventing abrupt variations in the presence of a non-uniform magnetic field. This distinction is particularly relevant in the context of the London equation, which establishes a *local* relationship between the supercurrent density $\mathbf{J}_s(\mathbf{r})$ and the vector potential $\mathbf{A}(\mathbf{r})$, requiring the $\mathbf{J}_s(\mathbf{r})$ to follow *exactly* any spatial variations in $\mathbf{A}(\mathbf{r})$. The coherence length sets a natural limit to this locality, representing the characteristic distance over which the vector potential must be averaged to determine the corresponding supercurrent density.

Any deviation from spatial uniformity incurs an additional kinetic energy cost, in other words, that any modulation of the superconducting wavefunction $\psi_s(\mathbf{k}, \mathbf{r})$ identified by it's momentum state $\mathbf{k}$ cost the system energy. Concretely, the increase of energy required for a modulation $\psi_s(\mathbf{k}, \mathbf{r}) \to \psi_s(\mathbf{k}+\mathbf{q}, \mathbf{r})$ with $|\mathbf{q}| \ll |\mathbf{k}|$ corresponds to $\delta E = \hbar^2|\mathbf{k}||\mathbf{q}|/2m$. However, if δE exceeds the superconductive energy gap E_g, superconductivity will be destroyed. The critical value $\mathbf{q}_0$ at which this happens is given $E_g = \hbar^2|\mathbf{k}_F||\mathbf{q}_0|/2m$ with k_F the momentum at the Fermi surface. We can then define an intrinsic coherence length ξ_0 related to this critical modulation as $\xi_0 = 1/q_0$ reading

$$\xi_0 = \frac{\hbar^2 k_F}{2mE_g} \tag{4}$$

As an additional complication, understand that both the coherence length ξ and the penetration depth λ of superconductors must be influenced by the mean free path of electrons ℓ_e in the normal state. For now we do not know their specific dependence on ℓ_e but we can at least guess for it qualitatively

by considering the nature of the electron's wavefunctions in disordered systems. In a so-called dirty superconductors, one that has a smaller mean free path of electrons, the wavefunction exhibits inherent spatial fluctuations due to disorder. This means that a localized variation in current density can be constructed with lower energy using these pre-existing wiggled wavefunctions, as opposed to the smoother wavefunctions found in a pure superconductor, where greater energy would be required to introduce similar variations. Hence, one can expect that $\xi < \xi_0$ for smaller ℓ_e. One the other hand, since the ability to screen an external magnetic field depends on how effectively the supercurrent can be set up across the sample. In the dirty limit the superconducting electrons will not be able to coordinate over long distances resulting in an overall weaker screening currents. Weaker screening means that the magnetic field penetrates deeper into the material, and thus one can also expect $\lambda > \lambda_0$ for smaller ℓ_e.

B. Ginzburg-Landau theory

Historically, the Ginzburg-Landau (GL) framework was introduced before the microscopic BCS theory of superconductivity. Although it was initially developed on largely phenomenological grounds, later work showed that it can be derived from the microscopic theory in certain limits. As a result, Ginzburg-Landau theory remains a cornerstone for describing superconductors near their critical temperature, providing both qualitative insights and quantitative tools for analyzing a wide range of superconducting phenomena.

Ginzburg-Landau theory offers a phenomenological way to understand how systems transition into the superconducting state building on the broader concept of second-order phase transitions at a given critical temperature. In this sense, one introduces an order parameter that captures how the system reorganizes itself at the threshold of the transition. This is analogous to how a ferromagnet spontaneously picks a magnetization $\mathbf{M}$ direction. When the system is in its non-magnetic state the magnetization is effectively zero, but as the temperature cools below a given critical temperature T_c (dubbed Curie temperature for the case of ferromagnets) it acquires a nonzero value.

Ginzburg-Landau theory clarifies the relationship between the two London's characteristic length scales—the penetration depth λ which quantifies how far magnetic fields can penetrate into the superconductor, and the coherence length ξ which quantifies how quickly the order parameter can change in space. The balance between these scales determines whether a material expels magnetic fields completely, dubbed type I superconductors, or admits them in quantized flux tubes, dubbed type II superconductors.

1. *Superconductive order parameter*

For superconductors, Ginzburg and Landau proposed that this order parameter is not just a simple number but a complex quantity that can vary in space, namely

$$\Psi(\mathbf{r}) = |\Psi(\mathbf{r})|e^{i\phi(\mathbf{r})} \tag{5}$$

whose magnitude $|\Psi(\mathbf{r})|$ and phase $\phi(\mathbf{r})$ convey key features of superconductivity. The effective number density of electrons n_s on the superconductive state is related to this magnitude, concretely $n_s = |\Psi(\mathbf{r})|^2$, and the current flowing locally at a given point $\mathbf{r}$ is related the gradient of the phase, concretely $|\boldsymbol{\nabla}\phi(\mathbf{r})|^2$. Intuitively you can think of the magnitude as how "strong" the superconductivity is while the phase is instead related to collective quantum behavior that underlies phenomena such as persistent currents and flux quantization. Moreover, since this order parameter is smoothly varying in space he needs not be uniform near boundaries or in the presence of impurities.

The Ginzburg-Landau theory is formulated by employing a minimization of the Helmholtz free energy density f_s (thermodynamic potential that measures the useful work that a system held at constant temperature can perform) in terms of $|\Psi(\mathbf{r})|^2$ and $|\nabla\Psi(\mathbf{r})|^4$ under constraints imposed by

external parameters such as temperature T and magnetic field $\mathbf{H}$ with respect to variations in the order parameter Ψ and the vector potential $\mathbf{A}$. Understand that you cannot have powers of $\Psi(\mathbf{r})$ in f_s because it must be real; nor can you just expand it terms of $\mathrm{Re}\{\Psi(\mathbf{r})\}$ since f_s must not depend on the absolute phase of $\Psi(\mathbf{r})$. Moreover, odd powers of $|\Psi(\mathbf{r})|^2$ are also excluded because they are not analytic at $\Psi(\mathbf{r}) = 0$.

As we will see, this procedure results in a set of coupled differential equations governing the behavior of the order parameter $\Psi(\mathbf{r})$, dubbed the 1st GL equation, and the electromagnetic vector potential $\mathbf{A}(\mathbf{r})$, dubbed the 2nd GL equation. This interplay between the spatially varying superconducting order parameter and the electromagnetic field lies at the heart of the Ginzburg-Landau description.

The fundamental GL postulate asserts that if the magnitude of order parameter is small and varies gradually in space (local electrodynamic approximation) then the Helmholtz free energy density f_s near the transition temperature T_c can be expanded into the power series expansion

$$\begin{aligned} f_s(T) &= f_{\text{normal}} + f_{\text{condensate}} + f_{\text{kinetics}} + f_{\text{magnetic}} \\ &= f_n + \left[\alpha(T)|\Psi(\mathbf{r})|^2 + \frac{\beta(T)}{2}|\Psi(\mathbf{r})|^4\right] + \frac{\hbar^2}{2m^*}\left|\left(\boldsymbol{\nabla} - \frac{ie^*}{\hbar c}\mathbf{A}(\mathbf{r})\right)\Psi(\mathbf{r})\right|^2 + \frac{H^2}{8\pi} \end{aligned} \tag{6}$$

with f_n the Helmholtz free energy density in the normal state, α and β some phenomenological parameters to be determined experimentally (in conventional BCS superconductors these parameters be derived from microscopic theory), e^* and m^* the effective charge and mass of the superconducting carriers respectively, $\mathbf{A}(\mathbf{r})$ the electromagnetic vector potential, and $\mathbf{B} = \nabla \times \mathbf{A}$ the external magnetic field magnitude. The 2nd and 3rd terms correspond to the condensation free energy density, allures to the fact that the superconducting state is to be more ordered than the normal state, the 4th term corresponds to the kinetic energy density of the charged superconducting carriers in the presence of a magnetic field leading to supercurrents (the 2nd of its term to be precise), and the 5th term to the energy density associated with the magnetic field itself.

Bulk solutions (absence of field and currents)

Deep inside the bulk of the superconductor, several London penetration length's in, if the system is at the critical temperature $T = T_c$ then the Helmholtz free energy density at the phase transition must be continuous, i.e that $f_s(T_c) - f_n(T_c) = \alpha(T_c)|\Psi_\infty|^2 + \beta(T_c)/2|\Psi(\Psi_\infty)|^4 \stackrel{!}{=} 0$, with Ψ_∞ the order parameter in the deep bulk regime notation. One the hand, minimizing f_s with respect to $|\Psi(\mathbf{r})|$, one obtains that

$$|\Psi_\infty|^2 \stackrel{!}{=} n_s^* = -\frac{\alpha}{\beta} \tag{7}$$

Substituting back into the previous condition one finds that

$$f_s(T_c) - f_n(T_c) = -\frac{\alpha(T_c)^2}{2\beta(T_c)} \equiv -\frac{H_c}{8\pi} \tag{8}$$

with H_c the critical magnetic field. See that the $\beta(T)$ parameter must always be positive, even if $\alpha(T) > 0$, because otherwise there would be a *finite* potential barrier that, if crossed, would result in infinite free energy. Oppositely, the $\alpha(T)$ parameter can take whatever value. If $\alpha(T) \geq 0$ the minimum free energy occurs at $|\Psi(\mathbf{r})| = 0$, corresponding to the normal state since $n_s = |\Psi(\mathbf{r})|^2$ states no density of electrons on the superconductive state. One the other hand, if $\alpha(T) < 0$ then the minimum free energy occurs at $|\Psi(\mathbf{r})| > 0$, corresponding to the superconductor state since it gives a lower free energy state. [see Fig.(1)].

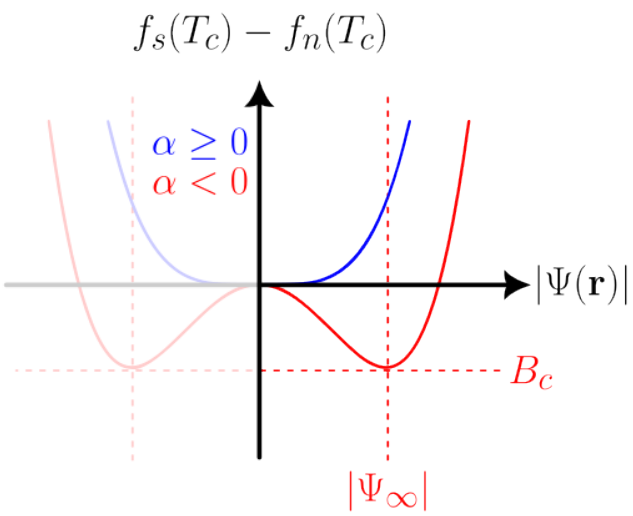

Figure 1. Ginzburg-Landau theory Helmholtz free energy density f_s

Temperature dependency

Since the $\alpha(T)$ must change from positive to negative at $T = T_c$ let us make a Taylor's series expansion around T_c but keeping only the linear term, reading $\alpha(t_s) = \alpha_s(1 - t_s)$ with $t_s = T/T_c$ and $\alpha_s < 0$, such that in the normal phase $T > T_c \Rightarrow t_s < 1 \Rightarrow \alpha(t_s) \propto \alpha_s < 0$ and in the superconducting phase $T < T_c \Rightarrow t_s > 1 \Rightarrow \alpha(t_s) \propto -\alpha_s > 0$. Inserting the empirical notations that $B_c \propto (1 - t_s^2)$ one can then infer deep that inside the bulk the temperature dependent behavior of the London's penetration length goes like $\lambda(t_s) \propto |\Psi_\infty(\alpha(t_s), H_c(t_s))|^2 \propto \left(1 - t_s^4\right)^{-1/2}$.

2. *Ginzburg-Landau equations*

Minimizing the total Helmholtz free energy density $F_s = \int_{\mathcal{V}} d^3\mathbf{r} f_s(\mathbf{r})$ over the volume $\mathcal{V}$ of the superconductive system with respect to the variation of the order parameter $\Psi^*(\mathbf{r})$ why the complex conjugate though? gives us the 1st Ginzburg-Landau equation

$$\alpha\Psi(\mathbf{r}) + \beta|\Psi(\mathbf{r})|^2\Psi(\mathbf{r}) + \frac{1}{2m^*}\left(-i\hbar\boldsymbol{\nabla}_\mathbf{r} - \frac{e^*}{c}\mathbf{A}\right)^2\Psi(\mathbf{r}) = 0 \tag{9}$$

See that, apart from the nonlinear term, this equation has the form of a Schrodinger equation for particles with energy eigenvalue $-\alpha$ within the same conditions. The nonlinear term acts like a repulsive potential of $\Psi(\mathbf{r})$ on itself, tending to favor wavefunctions $\Psi(\mathbf{r})$ which are spread out as uniformly as possible in space.

One the other hand, the variation of vector potential $\mathbf{A}$ gives us the 2nd Ginzburg-Landau equation

$$\mathbf{J}_s = \frac{e^*}{m^*}|\Psi(\mathbf{r})|^2\left(\hbar\boldsymbol{\nabla}_\mathbf{r}\phi(\mathbf{r}) - \frac{e^*}{c}\mathbf{A}(\mathbf{r})\right) \equiv e^*|\Psi(\mathbf{r})|^2\mathbf{v}_s \tag{10}$$

which shows us that also the superconductive current resembles quantum mechanical expressions in the same conditions, concretely the current of probability with the caveat of having an effective number density $n_s = |\Psi(\mathbf{r})|^2$, mass m^* and charge e^*. In the original formulation of the theory it was assumed without much thought that e^*, m^* and n_s^* corresponded to their normal electronic values however

experimental data surprisingly suggested a better fit for $e^* = 2e$, $m^* = 2m$ and $n_s^* = \frac{1}{2}n_s$. For us time travelers this obviously screams Cooper pairing of electrons as predicted by the microscopic BCS theory. See that the relation $\lambda = n_s e^2/m = n_s^* e^{*2}/m^*$ still holds though, ensuring that the London penetration depth remains unchanged due to the pairing mechanism. Notably, see that a decrease in the order parameter results in an increase in the penetration depth.

Choice of boundary conditions

As an additional and relevant detail, remember that along the variational procedure one must eventually provide a choice of boundary conditions of the superconductive volume. Indeed, in GL theory the boundary condition is that of an insulating surface such that it is ensured that no supercurrent leaks through the superconductor, i.e $\mathbf{J}_s \cdot \mathbf{n} = 0$ at the interface. Concretely, this means that $\left(-i\hbar\boldsymbol{\nabla}_{\mathbf{r}} - e^*/c\mathbf{A}(\mathbf{r})\right)\Psi(\mathbf{r})\big\rfloor_{\mathbf{n}} = 0$. From the microscopic theory de Gennes latter shown that the right side, rather then zero, should read instead $i\hbar/\Psi(\mathbf{r})b$ with b a real constant. If at the interface $\mathbf{A} = 0$ then b corresponds to the extrapolation length to the point outside the boundary at which Ψ would go to zero if it maintained the slope it had at the surface. The value of b will depend on the nature of the material to which contact is made, approaching $b = 0$ for a magnetic material and $b = +\infty$ for an insulator, with normal metals lying in between.

GL coherence length

Let us consider a simplified one-dimensional case were no magnetic field are present ($\mathbf{A} = 0$) and analyze GL 1st differential equation in Eq.(9). See that, in this case, $\Psi(\mathbf{r})$ get to be real since the equation only has real coefficients. Introducing the normalized wavefunction $\tilde{\Psi} = \sqrt{\beta/|\alpha|}\Psi$ with $\alpha = -|\alpha|$ the (one-dimensional) equation becomes $\xi^2\partial_x^2\tilde{\Psi} + \tilde{\Psi} - \tilde{\Psi}^3 = 0$ where we identified the characteristic length ξ of the order parameter variations as $\xi = \hbar^2/\left(2m^{*2}\left|\alpha(T)\right|\right)$. This is known as the GL coherence length which, as the name implies, plays the same role as the same as London's, describing the distance over which the superconductor can be represented by a wavefunction. Moreover, for my time-travelers fellows, this can also be understood as the distance over which Cooper pairs can be considered to be correlated. Within the deep bulk ($\mathbf{A} = 0$) the order parameter $\tilde{\psi}$ will not vary in space and thus one can solve the equation by setting the boundary conditions $\partial_x\tilde{\Psi} = 0$ and $\tilde{\Psi}^2 = 1$. One obtains

$$\Psi(x) = \sqrt{\frac{|\alpha|}{\beta}}\tanh\left(\frac{x}{\sqrt{2}\xi}\right) \tag{11}$$

3. Flux quantization

Consider a superconductor ring with a magnetic flux Φ passing through it's perforation inducing a persistent current $\mathbf{J}_s$ coursing trough it's "inner" "surface" as to counter act the magnetic field in the bulk within a penetration depth λ. Now, consider a circular path $\mathcal{C}$ within the deep bulk of the ring far away from any persistent currents, such that $\oint_{\mathcal{C}} \mathbf{J}_s \cdot d\boldsymbol{\ell} = 0$ with $\mathbf{J}_s$ given by the 2nd GL equation in Eq.(10). Since the system is defined at its minimal energy configuration the order parameter within the deep bulk Ψ_∞ must have a unique value at every point along the circular path. This leaves us specifically with $\oint_{\mathcal{C}} \mathbf{v}_s \cdot d\boldsymbol{\ell} = 0$ which is trivial to solve for. For the 1st term, one has that $\oint_{\mathcal{C}} \boldsymbol{\nabla}_{\mathbf{r}}\phi(\mathbf{r}) \cdot d\boldsymbol{\ell} = 2\pi n$, since $\phi(\mathbf{r})$ goes around in a circle and back to here it started acquiring a phase of 2π for each $n \in \mathbb{Z}$ lap, and for the 2nd term one obtain, by definition, the magnetic flux Φ, since $\oint_{\mathcal{C}} \mathbf{A}(\mathbf{r}) \cdot d\boldsymbol{\ell} = \oint_{\mathcal{S}} \boldsymbol{\nabla} \times \mathbf{A}(\mathbf{r}) \cdot d\mathbf{S} = \oint_{\mathcal{S}} \mathbf{B} \cdot d\mathbf{S} = \Phi$ with $\mathcal{S}$ the surface spanning the over the hole. Note that $n \neq 0$ requires that the contour cannot be contracted to a single point, meaning that the sample must always contain a hole, as it has in our case. Combining this results one obtains (with the foresight substitution $e^* = 2e$)

$$\Phi = n\frac{hc}{2e} \equiv n\Phi_0, \tag{12}$$

meaning that the flux through the ring is actually quantized in integral multiples of Φ_0, the flux quantum, also known as fluxoid. Bear in mind the subtlety that it's the total flux $\Phi = \Phi_s + \Phi_H$ that is quantized, i.e the sum of the flux from external magnetic field Φ_H and the flux from the from the persistent superconducting currents Φ_s. Since there is no quantization condition on the external sources then Φ_s itself must adjust appropriately in order that Φ assumes a quantized value.

GL coherence length

As a quick side note, see that putting together Eq.(8) and Eq.(7) along with London's penetration length definition in Eq.(3) and the fluxoid definition in Eq.(12) one can expresses the GL coherence length as

$$\xi(T) = -\frac{\Phi_0}{2\sqrt{2}\pi H_c(T)\lambda^*} \tag{13}$$

4. Type I and type II superconductors

As previously discussed, although currents can flow without any energy dissipation in superconductors, there are certain limitations; the material must operate below a given critical temperature T_c but also under magnetic field strengths below a critical value $H_c(T)$. With regard to their magnetic properties, particularly in the way they expelled magnetic fields superconductors can then be categorized into one of two types, simply named type I and type II.

On one hand, type I superconductors exhibit a sharp normal-superconductive phase transition with all magnetic flux being expelled while in the superconductive phase while type II superconductors exhibit an additional in-between "mixed state", also refereed to as "vortex state", where there is partial penetration of flux. This partial penetration occurs as a mechanism to minimize the overall magnetic energy. Surrounding these small localized regions of partial penetration —where the magnetic field is high enough to revert the superconductor into its normal phase—are circulating vortices of quantized screening currents that oppose the magnetic field guaranteeing that the material outside these regions remains in the superconducting state. This process by which superconductivity "kicks off" in small localized pockets is often referred to as nucleation. Understand that, although the sample is not locally superconducting in those regions, it can still have zero electric resistance as a whole since the currents predominantly flows through the superconducting areas. Moreover, understand that to maintain a lossless state these vortices must be pinned in place, for example, by defects within the crystal structure, or else they will move and generate a voltage leading to dissipation.

Another way to qualitatively understand this two types of superconductivity is by examining the interaction energy between superconducting vortices. Rather then performing a full explicit derivation, we can gain insight by considering the broader picture.

The derivation of the vortex interaction energy begins with determining the shape, and consequently the energy, of an individual vortex. This is realized by solving the field equations in cylindrical coordinates for a non-constant $\Psi(x)$, as we are dealing with local defects. In this choice of coordinates, the equations take the form of coupled nonlinear differential equations. An important detail in this derivation is that to compute the vortex energy per unit length, one must introduce a cutoff, which reflects the fact that a vortex can only exist within a finite-sized system.

Once the energy of the individual vortices is known, one goes to finds the energy of the entire system and then subtract them off to obtain the interaction energy between superconducting vortices. It reads $E_{\text{int}} \propto d/\lambda - \sqrt{2}d/\xi$ with d the distance between the vortices. This expression reveals two competing effects: a repulsive interaction caused by vortex currents circulating in opposite directions (analogous to the force between two parallel wires carrying currents in opposite directions) and an attractive interaction caused by the fact that a superconductor energetically favors a defect-free state, it tends to restore order by merging vortices whenever possible. The balance between these opposing forces determines whether vortices attract or repel. Quantitatively, what governs the nature of this interaction is the ratio between the GL coherence length $\xi(T)$ and London's penetration depth $\lambda(T)$, known as the

GL parameter $\kappa = \lambda(T)/\xi(T)$. See that apart from being a dimensionless quantity, since both $\lambda(T)$ and $\xi(T)$ diverge as $\sqrt{1-T/T_c}$ with temperature, κ is also temperature independent. If $\kappa > 1/\sqrt{2}$ the repulsive interaction dominates and thus the vortices repel from each other, arranging themselves into regular periodic structures, typically a triangular lattice. Since each vortex carries a quanta of flux Φ_0 this results in partial penetration of the magnetic field, a hallmark of type II superconductors. Conversely, if $\kappa > 1/\sqrt{2}$, the attractive interaction prevails, leading to the agglomerate and collapse of all vortices into a single entity. In this case, the superconductor has no mechanism to sustain flux penetration and instead exhibits the Meissner effect, a hallmark of type I superconductor.

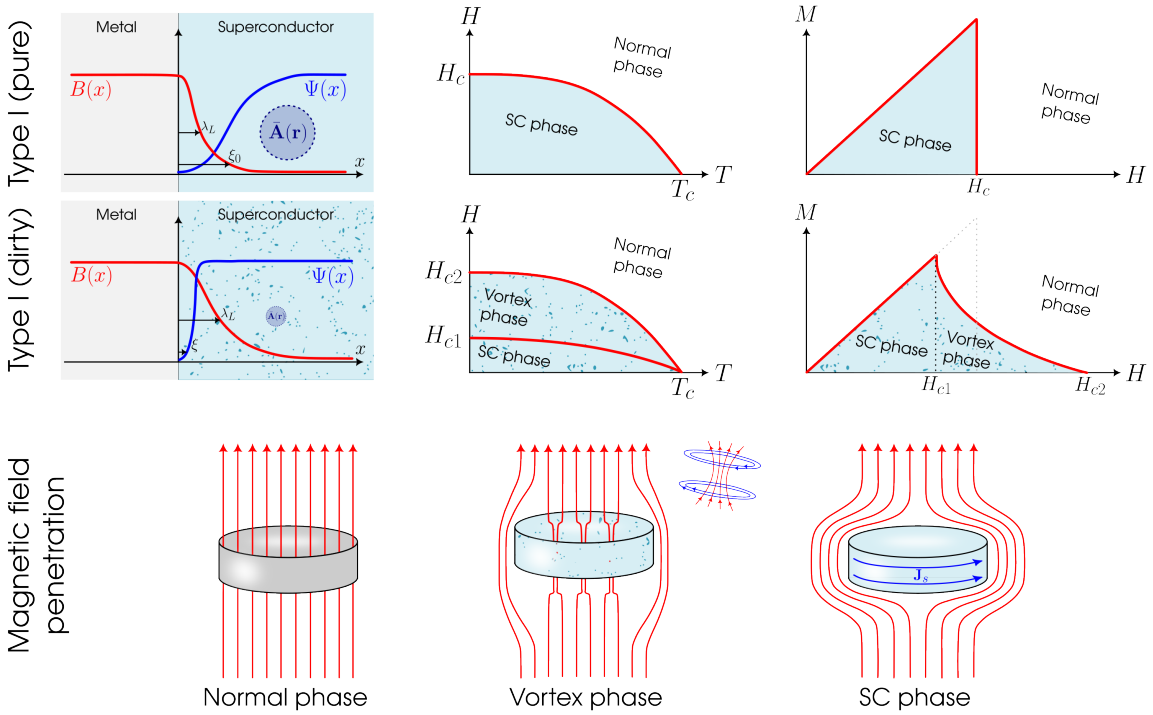

Figure 2. The nomenclature type I and type II will be made clear after Ginzburg-Landau theory, for now think of it as simply pure and dirty, respectively

5. *Little-Parks experiment*

Instead of the ring, consider now a superconducting cylindrical thin-film shell of radius R and thickness ℓ with a magnetic flux ϕ passing through its perforation. Specifically, we consider the shell to be so thin so that $\ell \ll \xi(T)$ with $\xi(T)$ the London's coherence length. In this case, any small deviation of $|\Psi(\mathbf{r})|$ would mean an excessively large $|\Psi(\mathbf{r})|^2$ contribution to the free energy which is not physically realistic. To correct this problem one then needs to approximate the magnitude to a uniform value, i.e $\Psi(\mathbf{r}) = \Psi_0$. In this conditions the Helmholtz free energy density f_s would approximately read $f_s^{\text{thin}} \approx f_n + (\alpha+\kappa)|\Psi_0|^2 + \beta/2|\Psi_0|^4 + H^2/8\pi$ with $\kappa = 1/2m^*v_s^2$ the kinetic energy of the superconducting current. Moreover, we further neglect the free energy term associated with the external magnetic field because it is is smaller than the kinetic energy by a ratio of πR^2 to

$1/\lambda^2$. The optimal value of $|\Psi_0|^2$ is then found by minimizing f_s^{thin} , for a given v_s, reading

$$|\Psi_0|^2 = \Psi_\infty \left[1 - \left(\frac{\xi(T) m^* v_s}{\hbar}\right)^2\right] \tag{14}$$

From the previews quantization condition $\Phi_s = n\Phi_0 - \Phi_H$ we already know what the supercurrent velocity v_s should be, it reads as the Φ_H/Φ_0-periodic function $v_s = \hbar/(m^* R)\,(n - \Phi_H/\Phi_0)$.

Let us analyze what happens at the normal-superconductor phase transitions. Substituting directly into Eq.(14) the supercurrent velocity v_s in it's Φ_H/Φ_0-periodic form and setting $|\Psi_0|^2 = 0$ one finds that, through the temperature dependence of the coherence length $\xi(T)$ in Eq.(**??**), there will be a periodic variation δT_c of the critical temperature T_c, concretely

$$\frac{\delta T_c(H)}{T_c} \propto \begin{cases} \dfrac{\xi_0^2}{R^2}\left(n - \dfrac{\Phi_H}{\Phi_0}\right)^2 & \text{for a pure SC} \\[2ex] \dfrac{\xi_0 \ell}{R^2}\left(n - \dfrac{\Phi_H}{\Phi_0}\right)^2 & \text{for a dirty SC} \end{cases} \tag{15}$$

This is known as the Little-Parks effect. See that the maximum of the depression of T_c occurs when $n - \Phi_H/\Phi_0 = 1/2$.

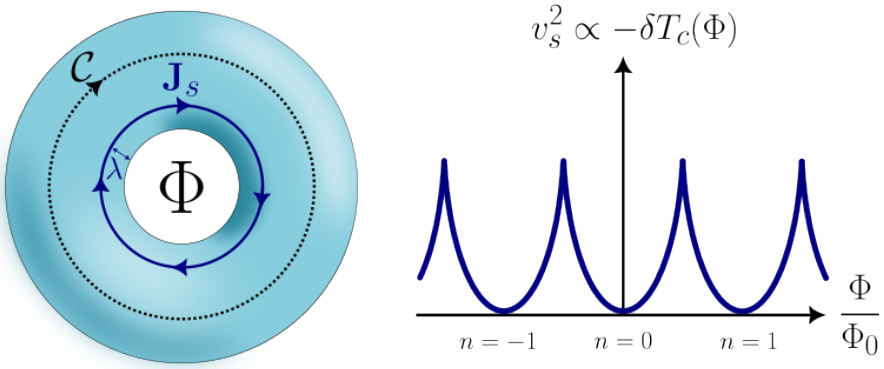

Figure 3. (left) fluxoid (right) Little-Parks effect

6. *Josephson effect*

7. *Time-dependent Ginzburg–Landau theory*

In equilibrium, the minimization of the free energy yields the lowest energy state for which the free energy does not change, to first order, with any variation of the order parameter or the fields. If, however, the system is not in an equilibrium state, the system should relax toward the equilibrium state. To account for the time-dependence of this relaxation process, the time-dependent Ginzburg-Landau (TDGL) equation is often used to describe the temporal behavior. The relaxation rate is assumed proportional to the variation of the free energy density with the order parameter Δ^*. The TDGL equation is written as

$$\left(i\hbar\frac{\partial}{\partial t} - 2\mu\right)\Psi = -\frac{i}{\tau_{\text{GL}}}\frac{\hbar}{|\alpha(T)|}\frac{\partial f_s}{\partial \Psi^*}, \text{ with } \quad \tau_{\text{GL}} = \frac{1}{16}\frac{1}{T_c - T} \tag{16}$$

the Ginzburg-Landau relaxation time and μ the chemical potential. The last expression, of course, equals zero in equilibrium, but is nonzero when displaced from equilibrium.

C. Bardeen–Cooper–Schrieffer theory

1. *Cooper pairing*

II. OVERVIEW OF SUPERCONDUCTIVITY REFINED THEORIES

A. Dirty superconductor theory

1. *Green's function formulation*

Gorkov invented a powerful methodology by deducing the equations of motion for the Green's functions. An anomalous Green's function, F, accounting for pair-correlations was introduced in addition to the normal electron Green's function. The two Green's functions form a closed set of equations, the solutions of which yield all the results of the BCS theory, and moreover, can be readily extended to incorporate dirty systems with impurities, as well as deal with nonlinearities, dynamics, and so on. Thus, type-II superconductors can readily be described. From the perspective of this text, the central importance of the Gorkov equations is the ultimate deduction of the Usadel equation for related Green's functions (to the Gorkov GF's), in the limit of dirty systems. The derivation of the Usadel diffusion equation was based on the works of Eilenberger and of Larkin and Ovchinnikov who independently applied the quasiclassical approximation to the Gorkov equations, and identified an energy-integrated version of the Gorkov Green's functions. These approaches led to a simplification of the Gorkov equations into Boltzmann transport-like equations for these modified Green's functions.

The Usadel diffusion equation is much more tractable and amenable to numerical implementations, enabling realistic experimental geometries and situations to be analyzed. In particular, issues of quasiparticle injection at the normal-superconductor interface, nonequilibrium quasiparticle distribution, and so on, are readily computed. These methodologies based on the Usadel equation are naturally suited to analyzing systems with 1D SC nanowires.

Abrikosov-Gorkov Green's Functions

Eilenberger–Larkin–Ovchinnikov equations

Usadel diffusion equation

2. *Path integral formulation*

B. p-wave superconductivity

III. CONCEPTS OF SYMMETRY AND TOPOLOGY

Topology studies whether objects can be transformed continuously into each other. In condensed matter physics we can ask whether the Hamiltonians of two different systems can be continuously transformed into each other. If that is the case, then we can say that two systems are 'topologically equivalent'.

In order to understand the concept of topology in condensed matter in the simplest way possible let us consider the transformation of a system described by the Hamiltonian $\mathcal{H}$ by the tuning of some external parameter α such that at $\mathcal{H}_i \equiv \mathcal{H}(\alpha = 0)$ is the initial state Hamiltonian and $\mathcal{H}_f \equiv \mathcal{H}(\alpha = 1)$ the final. Understand that the transformation of $\mathcal{H}$ most be physical, meaning that it should be just a matter of point of view. Because of this, not only must $\mathcal{H}$ be an hermitian matrix, i.e $\mathcal{H} = \mathcal{H}^\dagger$ (such that it has real eigenenergies), but also that any transformation must be isometric (aka norm-preserving) isomorphisms (aka one-to-one mapping). Due to Wigner's theorem these transformations can either be unitary $\mathcal{U}$ or anti-unitary $\bar{\mathcal{U}}$. A unitary transformation between two inner product spaces reads as $\langle \mathcal{U}\varphi | \mathcal{U}\psi \rangle = \langle \varphi | \psi \rangle$ while an anti-unitary transformation reads instead as $\langle \bar{\mathcal{U}}\varphi | \bar{\mathcal{U}}\psi \rangle = \langle \varphi | \psi \rangle^* = \langle \psi | \varphi \rangle$. Of course, any anti-unitary operator can be written as the product of a unitary operator and the complex conjugation operator $\mathcal{K}$.

Unitary transformations

Unitary transformations do not have particularly interesting consequences for topological classification. Consider an Hamiltonian $\mathcal{H}$ with the symmetry constraint $\mathcal{U}^\dagger \mathcal{H} \mathcal{U} = \mathcal{H}$. See that $\mathcal{H}$ commutes with $\mathcal{U}$ meaning that the system has a conservation law, and that the Hamiltonian can be brought to a block-diagonal form

$$\mathcal{H} = \left(\begin{array}{c|c} \mathcal{H}^{(1)} & \\ \hline & \mathcal{H}^{(2)} \end{array}\right) \text{ ,with } \mathcal{H}^{(n)} = \left(\begin{array}{c|c} h_{11} & h_{12} \\ \hline h_{12}^* & h_{22} \end{array}\right). \tag{17}$$

This procedure can be repeated until one runs out of unitary symmetries and is left with an irreducible block of the Hamiltonian, i.e. one which cannot be block diagonalized. In this case, every one of those $\mathcal{H}_i^{(n)}$ Hamiltonians at the n block-diagonal could be continuously deformed into $\mathcal{H}_f^{(n)}$, meaning that they are always topologically equivalent.

Introduction to CPT symmetries

One the other hand, anti-unitary transformations do impose constraints on an irreducible Hamiltonian, for example, by forcing it to maintain a (physically) finite energy gap, or to be a real matrix, or to be block off-diagonal. In this case, telling if $\mathcal{H}_i$ and $\mathcal{H}_f$ are topologically equivalent is not trivial. There are three fundamental discrete symmetries: chiral symmetry (CS) $\mathcal{C}$, parity symmetry $\mathcal{P}$, time-reversal symmetry (TRS) $\mathcal{T}$, known collectively as CPT symmetry. In a condensed matter picture, we often refer to the chiral symmetry as being a sublattice lattice and the parity symmetry as a particle-hole symmetry (PHS). Sublattice symmetry means that our system can be naturally split into two interpenetrating sublattices. The Hamiltonian connects only sites from these different sublattices and, as a result, it anticommutes with an operator that distinguishes between them. Particle-hole symmetry means that for every electronic state with energy ε there is a corresponding electron-hole (as in absence of an electron) state, at $-\varepsilon$. Hence, mirroring the electron's occupancy along the Fermi level, meaning that occupied becomes unoccupied and vice versa, the spectrum remains unchanged. Finally, time reversal symmetry means that our system would have behave the same if time flown backwards. In this backward time frame momentums change sign and spins flip.

There is, however, an important detail: both $\mathcal{T}$ and $\mathcal{P}$ are indeed anti-unitary transformations but $\mathcal{C}$ is not. This is because whenever a system has both TRS and PHS there is also a chiral symmetry $\mathcal{C} = \mathcal{P}\mathcal{T}$. This also means that if a system only has either but not both, it cannot have a chiral symmetry. In other words, the presence of any two out of the three symmetries implies that the third is also present. Since the product of two anti-unitary operators is a unitary operator then $\mathcal{C}$ must be unitary. Also, see that if both TRS and PHS are absent, then CS may or may not be present. In these two situations, formally known as *classes*, there are no anti-unitary symmetries, furthering their classification to *complex* classes.

Another important detail is that for TRS we have that $[\mathcal{H}, \mathcal{T}] = 0$ while for PHS we have that $\{\mathcal{H}, \mathcal{P}\} = 0$. By implication of what we just talked, also $\{\mathcal{H}, \mathcal{C}\} = 0$.

Furthermore, as the next and final note about this symmetries, know that TRS and PHS may come in two separate flavors, depending on whether they square to plus or minus one. So, for example, a system can behave in three ways concerning TRS: (1) it does not have TRS, (2) it has it and $\mathcal{T}^2 = +1$

(3) it has it and $\mathcal{T}^2 = -1$. On the other hand, the chiral symmetry only comes in one flavor, $\mathcal{C}^2 = +1$. Due to flavor combinations we find a total of 10 distinct symmetry classes displayed in Fig.(4). The classifications $\mathbb{Z}$, $2\mathbb{Z}$ and $\mathbb{Z}_2$ on the left are to be introduced in the following examples.

class	$\mathcal{C}$	$\mathcal{P}$	$\mathcal{T}$	$d=0$	1	2	3
A				$\mathbb{Z}$		$\mathbb{Z}$	
AI			1	$\mathbb{Z}$			
AII			−1	$2\mathbb{Z}$		$\mathbb{Z}_2$	$\mathbb{Z}_2$
AIII	1				$\mathbb{Z}$		$\mathbb{Z}$
BDI	1	1	1	$\mathbb{Z}_2$	$\mathbb{Z}$		
C		−1				$2\mathbb{Z}$	
CI	1	−1	1				$2\mathbb{Z}$
CII	1	−1	−1		$2\mathbb{Z}$		$\mathbb{Z}_2$
D		1		$\mathbb{Z}_2$	$\mathbb{Z}_2$	$\mathbb{Z}$	
DIII	1	1	−1		$\mathbb{Z}_2$	$\mathbb{Z}_2$	$\mathbb{Z}$

Figure 4. Symmetry periodic table with Altland-Zirnbauer classification. For more details on this table, for example, on how to go from $d = 0$ to $d > 0$ by adding and removing symmetries and it's Boot clock patterns see Akhmerov's "10 symmetry classes and the periodic table of topological insulators" at https://topocondmat.org/w8_general/classification.html.

It is important to have in mind that CPT symmetries may not be the only symmetries at play. Although these are the fundamental symmetries, if one works within a condensed matter framework, the underlying lattice will provide additional, often spatial, symmetries. These include, for example point group symmetries—inversion, mirror, and rotational symmetries—, and space group symmetries—translation, glide, or screw symmetries of the entire crystal lattice. Point group symmetries protect additional degeneracies or enforce selection rules that are not captured by the non-spatial discrete symmetries alone, for example, a mirror symmetry in a crystal that protects gapless modes on certain surfaces or edges that are invariant under reflection. One the other hand space group symmetries constrain the electronic band structure and can lead to phenomena like Dirac or Weyl points that interact with the superconducting pairing.

A. Introduction to topological invariants in 0D models

In order to study the effects of these symmetries, let us imagine a panoply of different systems and their energy spectrums as a function of α. Moreover, let us count the number of levels below zero energy (defined at the Fermi level ε_F) at each different α, denoting it with Q. This will be our topological invariant prototype. If Q is the same in the initial and final system and did not change along the tuning of α then there must be a continuous transformation Hamiltonian which does not close the gap. One the other hand, if Q changes then the system are *not* topologically equivalent as it would be needed to close the (physically real) gap. Hence, such a crossing changes the topological invariant, dubbed topological phase transition.

For all the examples that follow we assume a zero-dimensional ($d = 0$) system. In a condensed matter realization this could be, for instance, a quantum dot interaction will all kinds of external

systems. This will become

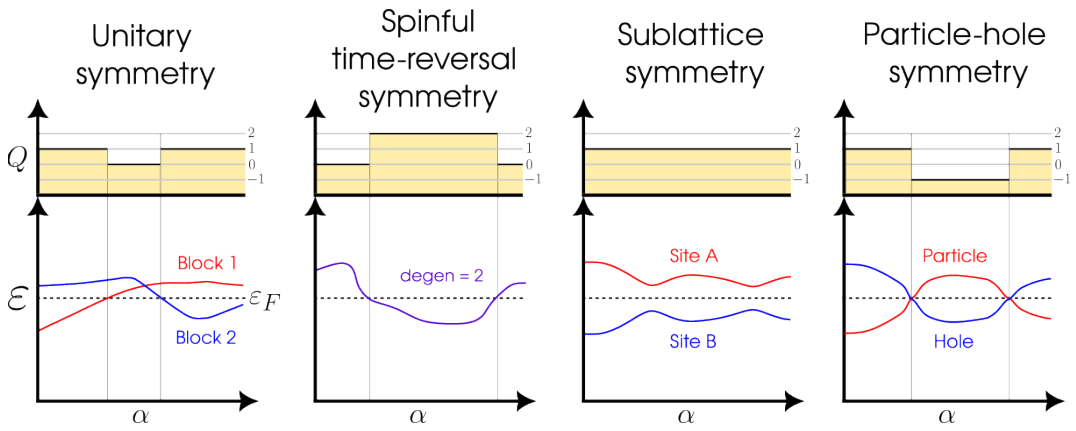

Figure 5. Kitaev chain Majorana modes pairing possibilities tbh I still don't fully undestand why I can't just change the Fermi energy? I mean, for the spinful TRS I could only get 0 or 2 still. Does the spectrum of the CS and PHS just translate along with ε_F while the unitary does not?

1. *Time-reversal symmetry*

Time-reversal symmetry is represented by an anti-unitary operator, and as such it can always be written as the product $\mathcal{T} = U\mathcal{K}$ with U an unitary matrix and $\mathcal{K}$ complex conjugation. A real Hamiltonian is a manifestation of time-reversal symmetry.

Spinless case

For example, for a spinless system we have $\mathcal{T} = \mathcal{K}$ and thus $\mathcal{T}\mathcal{H}\mathcal{T}^{-1} = \mathcal{H}^* = \mathcal{H}$ is a real matrix. In this case the TRS flavor is positive i.e $\mathcal{T}^2 = +\mathbb{1}$. Still, this case is also not interesting because is not different from the previous one, the different energy levels move and the topological invariant changes by one when one of them crosses zero. In this trivial case the topological invariant is an integer number, $Q = 0, \pm 1, \pm 2, \ldots \in \mathbb{Z}$. I mean, it should be $\mathbb{N}$ no? How would the negative numbers appear?

Spinful case

There is, however, a very important case where time-reversal symmetry makes a real difference. For a 1/2-spin system we the time-reversal operator reads $\mathcal{T} = i\sigma_y\mathcal{K}$ with $\sigma_y = \left[\begin{smallmatrix} 0 & -i \\ +i & 0 \end{smallmatrix}\right]$ the 2nd Pauli matrix (we reserve σ for Pauli matrices in spin orbital space). In this case the flavor is negative, i.e $\mathcal{T}^2 = -\mathbb{1}$, and $\mathcal{T}\mathcal{H}\mathcal{T}^{-1} = \sigma_y\mathcal{H}^*\sigma_y = \mathcal{H}$ meaning that every energy eigenvalue ε is doubly degenerate. This happens because both the electrons with spin up or down have the same eigenenergy. This doubly degeneracy is often refer to as Kramers' degeneracy. Such a Hamiltonian would read in matrix form as

$$\mathcal{H} = \left(\begin{array}{c|c} \varepsilon_1\mathbb{1} & M \\ \hline M^\dagger & \varepsilon_2\mathbb{1} \end{array}\right) = \left(\begin{array}{cc|cc} \varepsilon_1 & 0 & m_{11} & m_{12} \\ 0 & \varepsilon_1 & -m_{12}^* & m_{11}^* \\ \hline m_{11}^* & -m_{12} & \varepsilon_2 & 0 \\ m_{12}^* & m_{11} & 0 & \varepsilon_2 \end{array}\right). \tag{18}$$

with $\varepsilon_1, \varepsilon_2$ real numbers.

We can see the consequences of Kramers' degeneracy on the band spectrum versus α in Fig.(5). While the spectrum looks quite similar to the previous ones, whenever a line crosses zero energy, our topological invariant makes a jump of two, and not one! In this case, time-reversal symmetry constrains

the topological invariant to only take even values, $Q = 0, \pm 1, \pm 2, \ldots \in 2\mathbb{Z}$. This is an example of how topological properties can be influenced by discrete symmetries.

2. *Sublattice symmetry*

We just saw that time-reversal symmetry can forbid the topological invariant to take a certain set of values. We now study another case where a symmetry changes the topological properties dramatically.

Let's now take a system where we can split all the degrees of freedom into two groups—group A and group B—, such that the Hamiltonian only has nonzero matrix elements between two groups, and not inside each group. This situation arises naturally when the a given lattice has two sublattices. For example, for hexagonal boron nitrate (hBN) we can distinguish these sublattices as the boron and nitrogen sites respectively. The matrix of such an Hamiltonian would read

$$\mathcal{H} = \left(\begin{array}{c|c} & M \\ \hline M^\dagger & \end{array}\right) = \left(\begin{array}{cc|cc} 0 & 0 & m_{11} & m_{12} \\ 0 & 0 & m_{21} & m_{22} \\ \hline m_{11}^* & m_{21}^* & 0 & 0 \\ m_{12}^* & m_{22}^* & 0 & 0 \end{array}\right). \tag{19}$$

See that $\eta_z \mathcal{H} \eta_z = -\mathcal{H}$ where $\eta_z = [\,+1 \;\; 0\,;\; 0 \;\; -1\,]$ is the 3rd Pauli matrix (we reserve η for Pauli matrices in sublattice orbital space). This immediately means that if $\Psi = [\,\psi_A;\;\; \psi_B\,]^T$ is an eigenvector of the Hamiltonian with energy ε , then $[\,\psi_A;\;\; -\psi_B\,]^T$ is an eigenvector with energy $-\varepsilon$. A symmetric spectrum is the consequence of sublattice symmetry as seen in Fig.(5). This means that Q always stays constant and that we can always deform Hamiltonians with sublattice symmetry without closing the gap. This indicates that an extra symmetry, such as this one, may render the topology of a system as trivial.

3. *Particle-hole symmetry*

Another symmetry that has a strong influence on topology is the particle-hole symmetry, showing up in superconducting systems. As we saw in BCS theory, a superconductor will create(annihilate) pairs of electrons by breaking(forming) Cooper pairs costing a pairing energy of Δ to the system.

Let us consider that the dynamics of the electrons is described by the an hermitian H matrix while the pair creation and annihilation is described by an antisymmetric $\mathbf{\Delta}$ matrix. Understand that $\mathbf{\Delta}$ must antisymmetric just because because the fermion operators anticommute. The Hamiltonian describing the full system reads

$$\mathcal{H} = \left(\begin{array}{c|c} H & \mathbf{\Delta} \\ \hline -\mathbf{\Delta}^* & -H^* \end{array}\right) = \left(\begin{array}{cc|cc} h_{11} & h_{12} & 0 & \Delta \\ h_{12}^* & h_{22} & -\Delta & 0 \\ \hline 0 & -\Delta^* & -h_{11}^* & -h_{12}^* \\ \Delta^* & 0 & -h_{12} & -h_{22}^* \end{array}\right) \tag{20}$$

and is know as the Bogoliubov-de Gennes (BdG) Hamiltonian. Moreover, we now double the amount of degrees of freedom in the system by defining a Nambu spinors

$$\check{c}_i^\dagger = \begin{pmatrix} c_i^\dagger & c_i \end{pmatrix} \quad \text{and} \quad \check{c}_i = \begin{pmatrix} c_i \\ c_i^\dagger \end{pmatrix} \tag{21}$$

such that we can write

$$\check{\mathcal{H}} = \frac{1}{2}\check{c}^\dagger \mathcal{H}\check{c}.$$

This definitions indicates that the Bogoliubov-de Gennes Hamiltonian acts not only on electrons but also on an extra mirror set comprised of eletron-holes. Since holes are related to the electrons, $\mathcal{H}$ automatically inherits that extra symmetry. This symmetry exchanges electrons with holes, and has an anti-unitary operator $\mathcal{P} = \tau_x\mathcal{K}$ with $\tau_x = [\,0\;\;1\,;\;1\;\;0\,]$ the 1st Pauli matrix (we reserve σ for Pauli matrices in spin orbital space) and (as before) $\mathcal{K}$ complex conjugation. Hence we have that $\mathcal{P}\mathcal{H}\mathcal{P}^{-1} = -\mathcal{H}$. For this specific case it's flavor is positive, i.e $\mathcal{P}^2 = +\mathbb{1}$. Indeed, for every eigenvector $\Psi = [\,u;\;\;v\,]^T$ with energy ε, there will be a particle-hole symmetric eigenvector $\mathcal{P}\Psi = [\,v^*;\;\;u^*\,]^T$ with energy $-\varepsilon$. As clearly seen in Fig.(5), because of the minus sign in the particle-hole symmetry, the spectrum of $\mathcal{H}$ must be mirrored around zero energy, that is, the Fermi level).

Fermionic parity switches

See that this spectrum mirroring was also the case for sublattice symmetry however, in this case, energy levels do not repel around zero energy, so that crossings at zero energy appear. Unlike in the case of sublattice symmetry, a pair of $\pm\varepsilon$ energy levels does not corresponds to two distinct quantum states, but to a single quantum state. This quantum state is a coherent superposition of electrons and holes, a so called Bogoliubov quasiparticle. It has an excitation energy ε, and it is created by an operator $\gamma^\dagger = uc^\dagger + vc$. Populating the partner state at energy ε is the same as emptying the positive energy state.

In general a crossing between energy levels happens in the presence of a conserved quantity. While the mean-field Hamiltonian of a superconductor does not conserve the number of particles, it conserves the parity of this number. In other words, forming and breaking Cooper pairs does not affect whether the superconducting contains an even or odd number of electrons so fermion parity is a conserved quantity (provided that isolated electrons do not enter or leave the system). Fermion parity, however, is a many-body quantity, which cannot be directly described in terms of the single particle picture of the BdG Hamiltonian. This is why we had to double the number of degrees of freedom by hand. When a pair of levels crosses zero energy, the excitation energy ε of the Bogoliubov quasiparticle changes sign and it becomes favorable to add(remove) a Bogoliubov quasiparticle. In other words, at each crossing the fermion parity in the ground state changes from even to odd (or vice versa), meaning that these crossings are fermion parity switches.

The Pfaffian invariant

Since the ground state fermion parity is preserved by the superconducting Hamiltonian if there are no Bogoliubov quasiparticles crossing zero energy, the ground state fermion parity is the topological invariant of this system. It is clear however that this invariant is of a different nature than the one of the non-superconducting systems, which is given by the number Q of negative eigenvalues of the Hamiltonian. The latter cannot change for a BdG Hamiltonian, which has a symmetric energy spectrum, and hence it is not suitable to describe changes in fermion parity. For this kind of systems the actual topological invariant is called the *Pfaffian* and will either take the value $Q = \pm 1 \in \mathbb{Z}_2$ at every zero-energy crossing. Its rigorous definition is not really that important for our sake so we take a simpler approach.

In order to introduce the Pfaffian invariant, we start by making a basis transformation $\mathcal{H}'_{\text{BdG}} = \mathcal{U}\mathcal{H}_{\text{BdG}}\mathcal{U}^\dagger$ that makes the Hamiltonian an skew-symmetric matrix, i.e $\mathcal{H}^T = -\mathcal{H}$. We do this because the eigenvalues of antisymmetric matrices always come in pairs, i.e $\pm\varepsilon_n$. Further reasoning will become apparent as we go. Such a transformation is

$$H'_{\text{BdG}} = \frac{1}{2}\begin{pmatrix} 1 & 1 \\ i & -i \end{pmatrix} H_{\text{BdG}} \begin{pmatrix} 1 & 1 \\ i & -i \end{pmatrix} = \frac{1}{2}\left(\begin{array}{c|c} H - H^* + \Delta - \Delta^* & i\,(-H - H^* + \Delta + \Delta^*) \\ \hline i\,(+H + H^* + \Delta + \Delta^*) & H - H^* - \Delta + \Delta^* \end{array}\right)$$

Indeed, because H is Hermitian then $H - H^*$ is antisymmetric and $H + H^*$ is symmetric, i.e $\mathcal{H}^T = \mathcal{H}$; since Δ is antisymmetric then H'_{BdG} is also antisymmetric. In it's diagonalized form the determinant

of this matrix is just the product of the pairs of eigenenergies, i.e $\det(\mathcal{H}) = \prod_n \left(-\varepsilon_n^2\right)$. The key feature of the Pfaffian is revealed when taking now the square root of the determinant $\mathrm{Pf}(\mathcal{H}) = \sqrt{\det(\mathcal{H})} = \pm \prod_n i\varepsilon_n$. See that it is defined in such a way that the sign of the product is uniquely defined. At a fermion parity switch a single ε_n changes sign, so the Pfaffian changes sign as well while the determinant stays the same. We then define the actual topological invariant as

$$Q_{\mathrm{BdG}} = \mathrm{sign}\left[\mathrm{Pf}(i\mathcal{H})\right],$$

where we have included a factor of i just that the Pfaffian is a real number, such that at Q_{BdG} changes its value from $+1$ to -1 at every zero-energy crossing. This means that it is the correct expression for the ground state fermion parity and for the topological invariant. As some sort of intuition, you can think of it as if the number of holeonic levels below zero energy counts negatively to the overall positive electronic levels.

4. Combining symmetries

Particle-hole and spinful time-reversal symmetry

Take a system that has both particle-hole symmetry (PHS) and spinful time-reversal symmetry (TRS) described by the Hamiltonian $\mathcal{H}$. Let us take an intuitive approach to the band spectrum analysis. By PHS we know that an electronic band is equivalent to a negative holeonic band. On the other hand, by spinful TRS we know that there is Kramer degeneracy. Hence, since a PHS holeonic band counts as negative to the number of bands below zero energy we will always end up with Q being even and changing sign at a crossing. This is wrong but can't see the flaw in logic. I mean, looking at the table I can see that $P^2 = 1$ and $T^2 = -1$ gives me no constrain on Q and thus trivial topology.

B. Introduction to topological invariant in higher dimensions

In higher dimensional system the discrete energy levels of a $d = 0$ system are replaced by continuous energy bands defined along the Brillouin zone. In these higher dimensions the topological invariant cannot be defined merely as counting levels below the Fermi energy or by tracking sign changes of the Pfaffian in superconducting systems. Instead, the central theme of $d > 0$ dimensional band topology lies in the concept of geometric phases.

As an illustrative example of the concepts to come, consider a vector placed at the earth's north pole, always pointing in the tangent direction to the surface. If one translates the vector to the equator along a meridian, then along the equator for some distance, and back to the north pole, the vector's orientation will have changed relative to how it started by some angle. This angle is called the holonomy. The origin of non-trivial band topological properties is not so different from this example, with the crucial replacement of the vector by a Hamiltonian $\mathcal{H}(\boldsymbol{\alpha})$ depending on a set of parameters $\boldsymbol{\alpha} = (\alpha_1, ..., \alpha_N)$, and the earth a manifold (topological space that locally resembles Euclidean space near each point) spanned by those parameters. In the context of Hamiltonians, holonomy manifests as the acquisition of additional geometric phases by the eigenstate of $\mathcal{H}(\boldsymbol{\alpha})$ as the parameter space manifold is traversed. More concretely, in band topology, $\boldsymbol{\alpha}$ is taken to be the momenta $\mathbf{k} = (k_1, ..., k_d)$, with d the space dimensions, together with a set of additional tunable parameters (chemical potential, electric field, Zeeman, integrated out pairing, etc, etc...), and the eigenstate's additional geometric phase is the so-called Berry phases (we will further explore this later concept in just a moment). In this context, the restriction that evolution is adiabatic simply means that the system must remain in a situation where energy bands do not cross, i.e. the system must be gapped.

The idea is that if the parameters $\boldsymbol{\alpha}$ are varied adiabatically, then at each subsequent value of $\boldsymbol{\alpha}$, eigenstates of one set of parameters are smoothly deformed into another set. This is the content of

the adiabatic theorem, which states that in the case of adiabatic evolution of the parameters along a curve $\boldsymbol{\alpha}(t)$, the Schrodinger equation

$$-i\hbar\partial_t \left|\psi_n\left(\boldsymbol{\alpha}(t)\right)\right\rangle = \varepsilon_n\left(\boldsymbol{\alpha}(t)\right)\left|\psi_n\left(\boldsymbol{\alpha}(t)\right)\right\rangle \tag{22}$$

is obeyed instantaneously. Here$|\psi_n\left(\boldsymbol{\alpha}(t)\right)\rangle$ represents the eigenstate of the Hamiltonian $\mathcal{H}\left(\boldsymbol{\alpha}(t)\right)$ in the nth band with energy $\varepsilon_n\left(\boldsymbol{\alpha}(t)\right)$. Now, generically, due to the structure of the Schrodinger equation, and the normalization of states, a single degree of freedom exists, which can change the eigenstate as it is moved along the parameter space $\boldsymbol{\alpha}(t)$. This corresponds to a phase denoted by $\theta(t)$, such that the state can be decomposed as

$$\left|\psi\left(\boldsymbol{\alpha}(t)\right)\right\rangle = e^{i\theta(t)/\hbar}\left|\phi\left(\boldsymbol{\alpha}(t)\right)\right\rangle. \tag{23}$$

A short calculation performed by plugging this form of the state into the Schrodinger equation on both sides, and acting with $\langle\psi\left(\boldsymbol{\alpha}(t)\right)|$ on the left is enough to solve for the phase $\theta(t)$. One obtains

$$\theta(t) = \int_0^{t'} dt\left[\varepsilon\left(\boldsymbol{\alpha}(t)\right) + \frac{i}{\hbar}\left\langle\phi\left(\boldsymbol{\alpha}(t)\right)\right|\partial_t\left|\phi\left(\boldsymbol{\alpha}(t)\right)\right\rangle\right] \tag{24}$$

There are two contributions to the phase acquired by the eigenstate under adiabatic evolution. The first term is the familiar dynamical phase $\theta_D(t)$, which is acquired from evolving in time in the Hilbert space. However, a second term appears, namely

$$\gamma(t) = \frac{i}{\hbar}\int_0^{t'} dt\left\langle\phi\left(\boldsymbol{\alpha}(t)\right)\right|\partial_t\left|\phi\left(\boldsymbol{\alpha}(t)\right)\right\rangle$$

which is called the geometrical phase or Berry phase. This phase can be calculated via the aforementioned time integral, or equivalently by integrating over the curve $\mathscr{C}$ spanned in the parameter space α during the adiabatic evolution, reading

$$\gamma_{\mathscr{C}} = \int_{\mathscr{C}} d\boldsymbol{\alpha}\frac{i}{\hbar}\left\langle\phi(\boldsymbol{\alpha})\right|\nabla_{\boldsymbol{\alpha}}\left|\phi(\boldsymbol{\alpha})\right\rangle \equiv \int_{\mathscr{C}} d\boldsymbol{\alpha}\mathbf{A}(\boldsymbol{\alpha}) \tag{25}$$

with $A(\alpha)$ the so called Berry connection.

The Berry connection plays the same role in adiabatic evolution as the vector potential in electromagnetism, and indeed, much like in the latter theory, this connection can be used to construct a curvature tensor. In the context of electromagnetism, the curvature tensor is nothing but the electromagnetic tensor $F_{\mu\nu}$, while in the context of the adiabatic evolution of quantum systems, it is given the special name of Berry curvature $\Omega_{\mu\nu}$. Explicitly, this Berry curvature reads

$$\Omega_{\mu\nu}(\alpha) = \frac{\partial}{\partial\alpha^\mu}A_\nu(\alpha) - \frac{\partial}{\partial\alpha^\nu}A_\mu(\alpha)$$

One often considers the dual pseudo-vector to this tensor, this is $\Omega_{\mu\nu} = \varepsilon_{\mu\nu\xi}\boldsymbol{\Omega}^\xi$ with $\varepsilon_{\mu\nu\xi}$ the Levi-Civita symbol, and calls that the Berry curvature instead. This quantity is analogous to the magnetic field $\mathbf{B} = \nabla\times\mathbf{A}$. Another similarity between electromagnetism and these concepts is that the Berry connection, like the magnetic vector potential, is defined only up to a gauge choice. This makes it so the Berry phase is only well defined if closed curves $\mathscr{C}$ in the parameter space are considered.

As a final summary, information about the topology of the target space of $\mathcal{H}(\boldsymbol{\alpha})$ is acquired by integrating the Berry connection or curvature over the entire Brillouin zone, or in other words, the holonomy of the Hamiltonian as the Brillouin zone is traversed is sensitive to the band-topology. The integration of this Berry curvature yields quantities called topological invariants which are analogous to the Winding number of the Aharonov-Bohm effect (see the example below). In this $d > 0$ context, one can also refer to the topological invariants as Chern number.

A fundamental consequence of having a well-defined topological invariant in $d > 0$ is the so-called bulk-boundary correspondence. This principle asserts that nontrivial topological properties in the bulk of a material inevitably give rise to robust, gapless modes at its boundaries, whether along edges in 2D or surfaces in 3D. One can intuitively see why this should be the case by noting that at the boundary of a topological non-trivial system there is only vacuum, a topological trivial system. This means that, at this boundary, the topological invariant must change from something non-zero to zero which is only possible if the gap closes. This gives rise to emergent gapless edge state which are protected against perturbations that do not close the bulk gap.

1. Aharonov-Bohm effect

As a predecessor to the topological band theory, we now introduce the reader to an electromagnetism examples known as the Aharonov-Bohm (A-B) effect as a starting point to understanding the Berry phase, connection, curvature in more detail.

Consider an electron whose movement is restricted to the $x\mathcal{O}y$ place where an infinitely thin and long solenoid pierces through it at it's center. Inside the solenoid an electric current flow inducing a magnetic field $\mathbf{B} = B\hat{z}$ such that a magnetic flux ϕ flows penetrates the the plane of motion of the electron. Although there exists no field or flux outside the solenoid, a magnetic vector potential $\mathbf{A}$ permeates all space. Now, note that the electron wandering the plane will actually be affected by the vector potential, in that the Hamiltonian describing it will have the form

$$\mathcal{H}(\mathbf{r}) = \frac{\hbar^2}{2m}\left(\boldsymbol{\nabla}_{\mathbf{r}} - e\boldsymbol{\nabla}_{\mathbf{r}} \cdot \mathbf{A}(\mathbf{r})\right)^2 \tag{26}$$

with $\mathbf{p} = -i\hbar\boldsymbol{\nabla}_{\mathbf{r}}$ the momentum operator, e the electron charge and m its mass. In this case, the parameters $\boldsymbol{\alpha}$ can be identified with the actual position of the electron $\mathbf{r}$. Since the electron cannot enter the solenoid, which is assumed to be placed at $\mathbf{r} = 0$, its movement is restricted to everywhere except there.

As explain in the previous section, as the electron moves following a curve $\mathscr{C}$ it will acquire a Berry phase, or rather, is in this context, the A-B phase, given by Eq.(25) as

$$\gamma_{\text{A-B}} = \frac{e}{\hbar}\oint_{\mathscr{C}} d\boldsymbol{r}\mathbf{A}(\boldsymbol{r}), \tag{27}$$

with $\mathbf{A}$ being not the general Berry connection but the actual physical vector potential. The A-B phase, in some sense, measures the inability of making a continuous gauge choice for the magnetic vector potential in a punctured plane. The presence of the puncture hole makes it so a discontinuity along a branch cut is a mathematical necessity, and as a result, if an electron loops around the hole, it will acquire a non-trivial phase, dependent only on the number of times it goes around the hole (see Fig. 6). For this reason, it is said that the A-B phase is a topological quantity, depending only on the topology of the electron's trajectory, namely on a quantity called the winding number.

Alternatively, through the usage of Stoke's theorem, it is simple enough to compute the A-B phase as being proportional to the magnetic flux, this is

$$\gamma_{\text{A-B}} = \frac{e}{\hbar}\iint d\mathcal{S}\cdot\mathbf{B} = \frac{e}{\hbar}W\phi$$

enclosed by the trajectory's area $\mathcal{S}$, where $W \in \mathbb{Z}$ counts the number of loops the electron makes around the solenoid. It's precisely this quantity that corresponds precisely to the winding number.

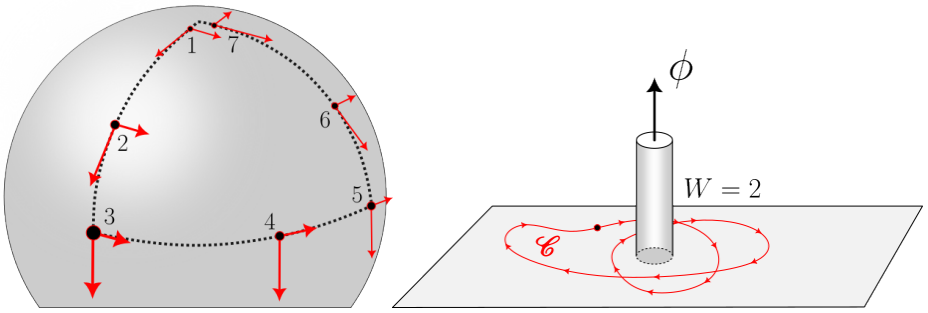

Figure 6. **(a)** Holonomy, **(b)** Aharonov-Bohm effect

2. *Quantum Thouless pump*

IV. TOPOLOGICAL SUPERCONDUCTIVITY IN 1D MODELS

A. Kitaev model

The *Kitaev chain* or *Kitaev–Majorana chain* is a toy model for a \topological superconductor using a 1D hybrid (semiconductor+superconductor) nanowires featuring Majorana bound states. It consists of a 1D linear lattice of N site and spinless fermions at zero temperature, subjected to nearest neighbor hoping interactions. The real-space tight-binding Hamiltonian describing such model reads

$$H = \mu \sum_{i=1}^{N} \left(c_i^\dagger c_i - \frac{1}{2} \right) - t \sum_{i=1}^{N-1} \left(c_{i+1}^\dagger c_i + h.c \right) + \Delta \sum_{i=1}^{N-1} \left(c_{i+1}^\dagger c_i^\dagger + h.c \right) \tag{28}$$

with $c_i^\dagger$ (c_i) fermionic creation (annihilation) operators, μ the chemical potential, t the hopping energy and Δ an proximity induced superconducting p-wave pairing.

The objective of this model definition is to be able to have a Majorana bound states on the edges mode. For this, let us engineering the Hamiltonian in such a special way that it is actually possible to separate two Majoranas. Foremost, we define each site n as if it has two sublattices, $s = A$ and $s = B$. We then define Majorana operators relating to the fermionic operators as

$$\gamma_i^A = c_i^\dagger + c_i \qquad \text{and} \qquad \gamma_i^B = i \left(c_i^\dagger - c_i \right) \tag{29}$$

or rather, in the opposite way, as

$$c_i^\dagger = \frac{1}{2} \left(\gamma_i^A - i\gamma_i^B \right) \qquad \text{and} \qquad c_i = \frac{1}{2} \left(\gamma_i^A + i\gamma_i^B \right) \tag{30}$$

Indeed, each site can host a fermion or, equivalently, each site hosting two Majorana modes. These Majorana operators are Hermitian $\gamma_i^s = (\gamma_i^s)^\dagger$, unitary $(\gamma_i^s)^2 = 1$ and anticommute as $\left\{ \gamma_i^s, \gamma_j^{s'} \right\} = 2\delta_{ij}\delta_{ss'}$.

Substituting directly into the Hamiltonian of Eq.(28) the fermionic operators as given by Eqs.(30) we obtain

$$H = -i\mu \frac{1}{2} \sum_{i=1}^{N} \gamma_i^B \gamma_i^A + i \frac{1}{2} \sum_{i=1}^{N-1} \left(\omega_+ \gamma_i^B \gamma_{i+1}^A + \omega_- \gamma_{i+1}^B \gamma_i^A \right), \quad \text{with } \omega_\pm = \Delta \pm t \tag{31}$$

From it we can distinguish between two phases—trivial and topological—, corresponding, respectively, to two different ways of pairing these Majoranas states—no unpaired modes or one isolated mode on both edges. These pairing configuration are depicted in Fig.7 in blue and red respectively. This phases can be easily identified, respectively, in their limiting regimes where one sets $\Delta = t = 0$ and $\mu = 0$ with $\Delta = t \neq 0$.

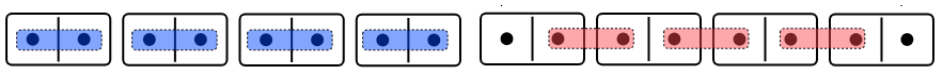

Figure 7. Kitaev chain Majorana modes pairing possibilities

Indeed, see that by setting $\Delta = t = 0$ within the Hamiltonian of Eq.(31) we obtain

$$H_{\text{trivial}} = -i\mu\frac{1}{2}\sum_{i=1}^{N}\gamma_i^B\gamma_i^A, \tag{32}$$

which corresponds to the limiting case of "no unpaired Majorana modes" configuration. The energy cost for each fermion to be occupied is μ, with all excitations having an energy of either $\pm\mu/2$. The band structure will then have a gapped bulk and no zero energy edge states. Furthermore, see that the wavefunctions of the first three energy states shown in Fig.(8).(middle) in this trivial phase simply resemble the harmonic modes of a string states.

On the other hand, see that by setting $\mu = 0$ with $\Delta = t \neq 0$ we obtain

$$H_{\text{topological}} = it\sum_{n=1}^{N-1}\gamma_i^B\gamma_{i+1}^A \tag{33}$$

which corresponds to the "unpaired edge Majorana mode" configuration where every Majorana operator is coupled to a Majorana operator of a different kind in the next site. Note that the summation only goes up to $n = N - 1$. Moreover, see that by assigning a new fermion operator $\tilde{c}_i = 1/2\left(\gamma_i^B + i\gamma_{i+1}^A\right)$, the Hamiltonian can be otherwise expressed as

$$H_{\text{topological}} = 2t\sum_{n=1}^{N-1}\left(\tilde{c}_i^\dagger\tilde{c}_i + \frac{1}{2}\right) \tag{34}$$

which describes a new set of $N-1$ Bogoliubov quasiparticles with energy t. For every Majorana pair we assign an energy difference $2t$ between the empty and filled state. All states which are not at the ends of the chain have an energy of $\pm t$ and thus the bands structure has a gapped bulk. However, see that the missing mode $\tilde{c}_N = 1/2\left(\gamma_N^B + i\gamma_1^A\right)$, which couples the Majorana operators from the two endpoints of the chain, does not appear in the Hamiltonian and thus it most have zero energy. As the presence of this mode does not change the total energy, the ground state is two-fold degenerate. This condition is a topological superconducting non-trivial phase. This mode is called a Majorana zero mode and is highly delocalized at the edges, as it can be seen in red in Fig(8).(middle). As one tunes μ in the direction of the trivial phase, the topological gap, protected by particle-hole symmetry (PHS), gets smaller and smaller and the Majoranas wavefunctions stay less and less localized at the edges. At the transition between the trivial and topological, when the chemical potential takes it's critical value of $|\mu| = 2t$, the first energy states stays evenly distributed along the chain.

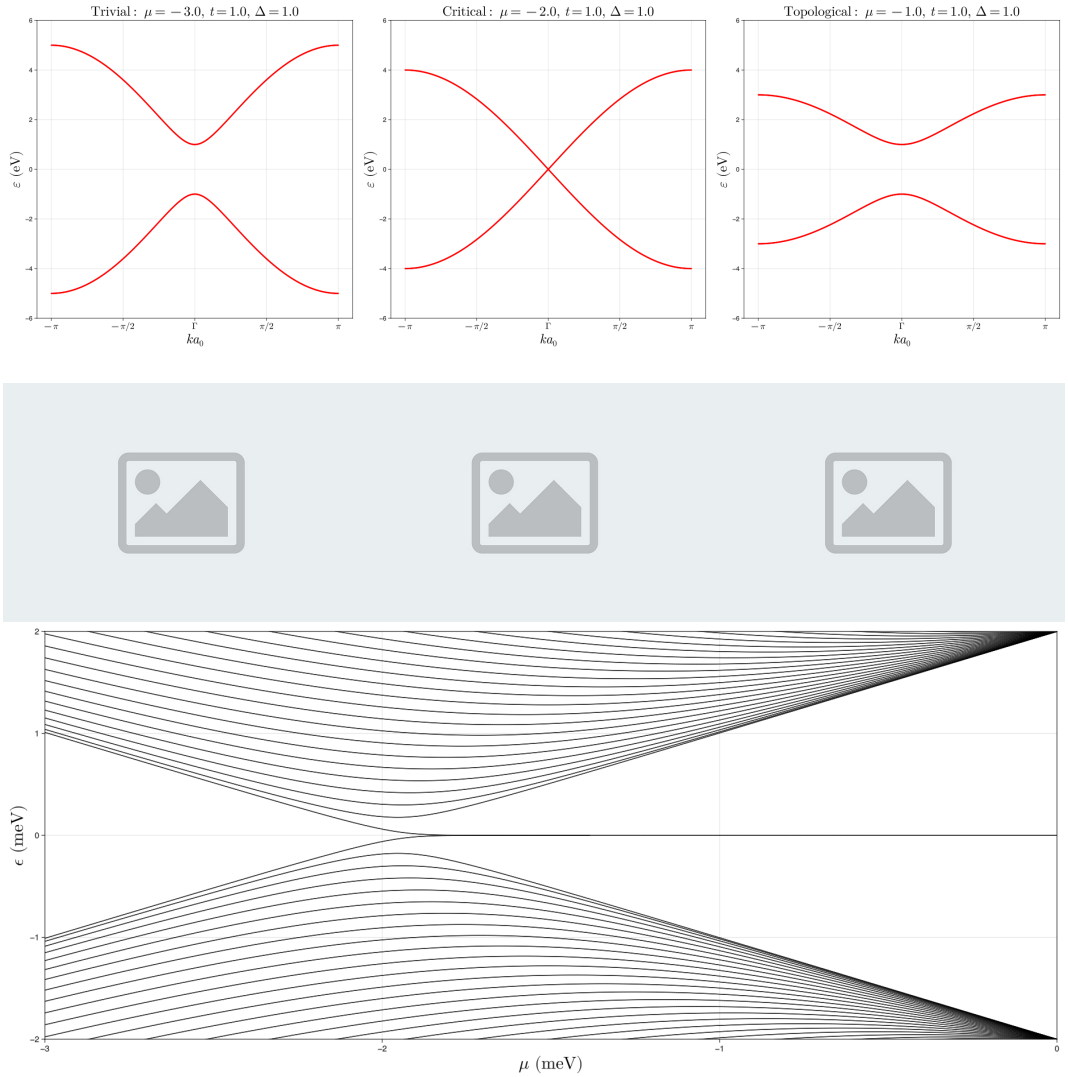

Figure 8. Kitaev chain **(top)** band structure **(middle)** I will eventually plot the 1st, 2nd and 3rd state wavefunction here at each regime, and **(bottom)** band spectrum for a chain length of $L = 50$ with lattice spacing $a_0 = 1$ fixing $\Delta = t = 1.0$. The critical μ shifts forward to infinity as $L \to 0$.

Bogoliubov-de Gennes Hamiltonian Let us now define the Hamiltonian in E.(28) in its Bogoliubov-de Gennes (BdG) form

$$H = \frac{1}{2}\check{c}^\dagger H_{\text{BdG}}\check{c}.$$

where we have defined the Nambu spinor as

$$\check{c}_i^\dagger = \begin{pmatrix} c_i^\dagger & c_i \end{pmatrix} \quad \text{and} \quad \check{c}_i = \begin{pmatrix} c_i \\ c_i^\dagger \end{pmatrix} \tag{35}$$

This proves not only useful to the study of the system's symmetries, but it also a necessary step for the numerical implementation in *Quantical.jl*. Defining τ_x, τ_y, τ_z as Pauli matrices in the particle-hole

subspace and using we the fermionic anti-commutation properties $\{c_i, c_j^\dagger\} = \delta_{ij}$ and $\{c_i, c_j\} = 0$, one can check that

$$\mu: \quad \check{c}_i^\dagger \tau_z \check{c}_i = \begin{pmatrix} c_i^\dagger & c_i \end{pmatrix} \begin{pmatrix} 1 & 0 \\ 0 & -1 \end{pmatrix} \begin{pmatrix} c_i \\ c_i^\dagger \end{pmatrix} = c_i^\dagger c_i - c_i c_i^\dagger = 2c_i^\dagger c_i - 1 \tag{36}$$

$$t: \quad \check{c}_j^\dagger \tau_z \check{c}_i = \begin{pmatrix} c_j^\dagger & c_j \end{pmatrix} \begin{pmatrix} 1 & 0 \\ 0 & -1 \end{pmatrix} \begin{pmatrix} c_i \\ c_i^\dagger \end{pmatrix} = c_j^\dagger c_i - c_j c_i^\dagger = c_j^\dagger c_i + h.c \tag{37}$$

$$\Delta: \quad \check{c}_j^\dagger i\tau_y \check{c}_i = \begin{pmatrix} c_j^\dagger & c_j \end{pmatrix} \begin{pmatrix} 0 & 1 \\ -1 & 0 \end{pmatrix} \begin{pmatrix} c_i \\ c_i^\dagger \end{pmatrix} = c_j^\dagger c_i^\dagger - c_j c_i = c_j^\dagger c_i^\dagger + h.c \tag{38}$$

Hence the Hamiltonian in Eq.(28) in its BdG form reads as

$$H = \mu \frac{1}{2} \sum_i \check{c}_i^\dagger \tau_z \check{c}_i - t \sum_{i=1}^{N-1} \check{c}_{i+1}^\dagger \tau_z \check{c}_i + \Delta \sum_{i=1}^{N-1} \check{c}_{i+1}^\dagger i\tau_y \check{c}_i \tag{39}$$

See that the Hamiltonian has particle-hole symmetry, i.e $\mathcal{P}H\mathcal{P}^{-1} = -\tau_x H^* \tau_x = -H$ with $\mathcal{P} = \tau_x \mathcal{K}$ and $\mathcal{K}$ complex conjugation, as well as time reversal symmetry, i.e $\mathcal{T}H\mathcal{T}^{-1} = H^* = H$ with $\mathcal{T} = \mathcal{K}$ for this spinless case (for reference, $\mathcal{T} = i\sigma_y \mathcal{K}$ for a 1/2-spin system). Once again, to understand why this is the case check.

Topological invariant

1. *Majorana modes at a domain wall*

Consider the case where we weld together two semi-infinite nanowires with one in it's trivial phase and the other in it's trivial phase. The spacial profile of the chemical potential $\mu(x)$ would then approximately a Heaviside theta function from $|\mu_{\text{left}}| > 2t$ to $|\mu_{\text{right}}| < 2t$, forming a doping domain wall at it's center. Hamiltonian wise, one just substitutes $\mu \to \mu(x)$ directly into Eq.(28). What one obtains in this situation is a Majorana mode localized at the domain wall with its twin forming in the semi-infinite edge of the topological side.

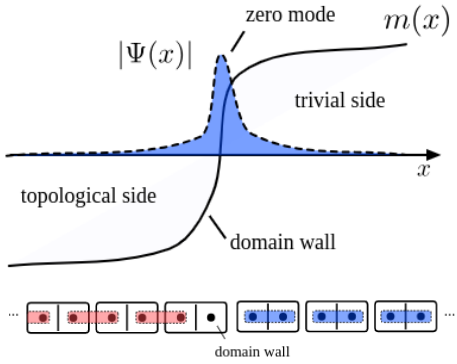

Figure 9. needs caption

2. Kitaev ring

B. SSH model

The most relevant references used for this section follow:

C. Oreg-Lutchyn models

The Oreg-Lutchyn Majorana minimal model consists of a finite 1D semiconductor (SM) nanowire with strong spin-orbit coupling (SOC) α and a tunable chemical potential μ, in proximity of a superconductor (SC) of homogeneous pairing Δ, having a magnetic field B_z applied along it's length, defined as the $\hat{z}$ direction. The Rashba effect describes the coupling of an electric field E_x that breaks inversion symmetry breaking in the direction perpendicular to the wire, to the electron's spin, i.e $\propto (i\vec{\nabla} \times \hat{x}) \cdot \vec{\sigma} = i\sigma_y \partial_z$ with $\vec{\sigma} = (\sigma_x, \sigma_y, \sigma_z)$. The Zeeman effect described the spin splitting due to the in-plane magnetic field B_z. The pairing term describes the Cooper pairs from BCS theory than could tunnel from the SM to the SC.

The tight-binding Hamiltonian describing such system can then be decomposed as

$$H = H_{\mathrm{K}} + H_{\mathrm{SOC}} + H_{\mathrm{Z}} + H_{\mathrm{SC}} \tag{40}$$

$$H_{\mathrm{K}} = (2t - \mu) \sum_{i\sigma} c^{\dagger}_{i\sigma} c_{i\sigma} - t \sum_{\langle i,j \rangle \sigma} c^{\dagger}_{i\sigma} c_{j\sigma} \tag{41}$$

$$H_{\mathrm{SOC}} = \frac{\alpha}{2a_0} \sum_{i\sigma} \left(c^{\dagger}_{i+1\bar{\sigma}} c_{i\sigma} + h.c \right) \tag{42}$$

$$H_{\mathrm{Z}} = V_{\mathrm{Z}} \sum_{i} \left(c^{\dagger}_{i\uparrow} c_{i\uparrow} - c^{\dagger}_{i\downarrow} c_{i\downarrow} \right) \tag{43}$$

$$H_{\mathrm{SC}} = \Delta \left(c^{\dagger}_{i\downarrow} c^{\dagger}_{i\uparrow} + \mathrm{h.c.} \right) \tag{44}$$

with $c^{\dagger}_i$ (c_i) fermionic creation (annihilation) operators, μ the chemical potential, $t = \eta / a_0^2$ the hopping energy into $\langle i, j \rangle$ nearest-neighbouring sites with a_0 the lattice constant and $\eta = \hbar^2 / 2m^*$ with m^* the effective mass of the electrons, $V_{\mathrm{Z}} = g_J \mu_{\mathrm{B}} B_z / 2$ the Zeeman potential with g_J the Landé gyromagnetic moment and μ_{B} Bohr's magneton, α the Rashba SOC strength and Δ proximity induced superconducting s-wave pairing.

A paragraph explaining the bands.

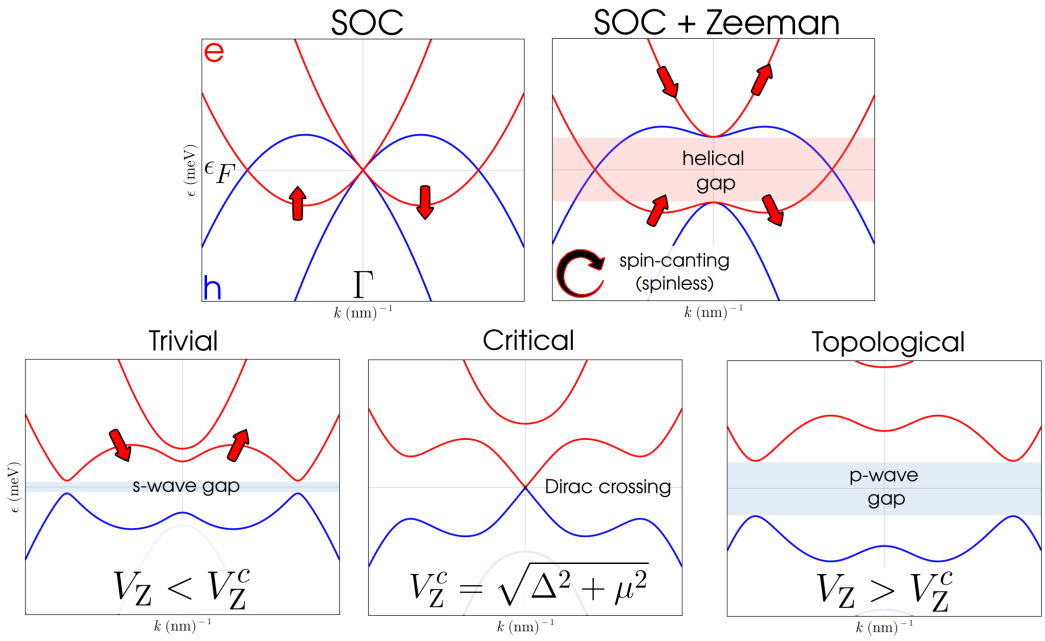

Figure 10.

A paragraph explaining the phase-diagram, pfaffian and band spectrum.

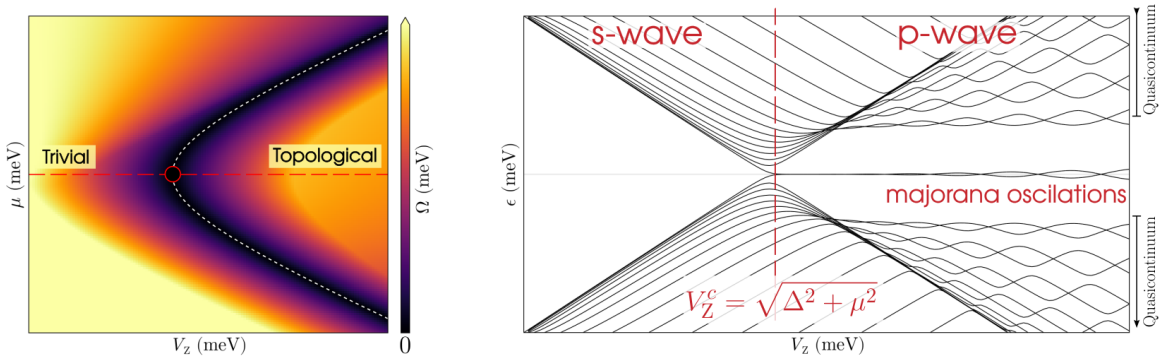

Figure 11.

Bogoliubov-de Gennes Hamiltonian Shown below are the broad strokes of a numerical implementation of the Hamiltonian in Julia using the Quantica.jl. However, prior to this implementation, we will be needing the Bogoliubov-de Gennes formalism. For this, need to double the degrees of freedom through the Nambu-spinor. In the so called unrotated-spin basis we define a Nambu spinor as

$$\check{c}_i^\dagger = \begin{pmatrix} c_i^\dagger & c_i \end{pmatrix} = \begin{pmatrix} c_{i\uparrow}^\dagger & c_{i\downarrow}^\dagger & c_{i\uparrow} & c_{i\downarrow} \end{pmatrix} \tag{45}$$

In this Nambu⊗spin orbital space the Hamiltonian in Eq.(40) reads

$$H = H_{\mathrm{K}} + H_{\mathrm{SOC}} + H_{\mathrm{Z}} + H_{\mathrm{SC}} \tag{46}$$

$$H_{\mathrm{K}} = (2t-\mu)\sum_i \check{c}_i^\dagger[\tau_z\otimes\sigma_0]\check{c}_i - \frac{1}{2}t\sum_{\langle i,j\rangle}\check{c}_i^\dagger[\tau_z\otimes\sigma_0]\check{c}_j \tag{47}$$

$$H_{\mathrm{SOC}} = \frac{\alpha}{2a_0}\sum_i \check{c}_i^\dagger[\tau_z\otimes i\sigma_y]\check{c}_{i+1} \tag{48}$$

$$H_{\mathrm{Z}} = V_Z\sum_i \check{c}_i^\dagger[\tau_z\otimes\sigma_z]\check{c}_i \tag{49}$$

$$H_{\mathrm{SC}} = \frac{1}{2}\Delta\sum_i \check{c}_i^\dagger[\tau_y\otimes\sigma_y]\check{c}_i \tag{50}$$

with τ Pauli matrices in the particle-hole subspace and σ in the spin subspace.

To understand why this is the case check we show explicitly the derivation for the pairing term as an example. It reads:

$$\begin{aligned}\check{c}^\dagger[\tau_y\otimes\sigma_y]\check{c} &= \begin{pmatrix} c_\uparrow^\dagger & c_\downarrow^\dagger & c_\uparrow & c_\downarrow \end{pmatrix}\left(\begin{array}{cc|cc} 0 & 0 & 0 & -1 \\ 0 & 0 & +1 & 0 \\ \hline 0 & +1 & 0 & 0 \\ -1 & 0 & 0 & 0 \end{array}\right)\begin{pmatrix} c_\uparrow \\ c_\downarrow \\ c_\uparrow^\dagger \\ c_\downarrow^\dagger \end{pmatrix} \\ &= -c_\uparrow^\dagger c_\downarrow^\dagger + c_\downarrow^\dagger c_\uparrow^\dagger + c_\uparrow c_\downarrow - c_\downarrow c_\uparrow = 2\left(c_\downarrow^\dagger c_\uparrow^\dagger + \mathrm{h.c.}\right)\end{aligned} \tag{51}$$

where we the fermionic anti-commutation properties $\{c_i, c_j^\dagger\} = \delta_{ij}$ and $\{c_i, c_j\} = 0$.
The remaining terms derivation is analogous but even simpler because there is will be no mixing of particle with particle-hole components; the holeonic terms will correspond to the negative of the electronic terms, meaning that one just needs to expand the space according to $\tau_z\otimes$ the respective spin matrix. For the kinetic term there is no mixing of spin so it must trivially have the spin Pauli matrix σ_0. Similarly, for the Zeeman term there is only the same-spin mixing of the type $\uparrow\uparrow - \downarrow\downarrow$ so it must have σ_z . As for the SOC term there is spin-mixing of opposing spins, so the options are either σ_x or $i\sigma_y$ (with a i for it to be hermitian). One can check with the fermionic anti-commutation properties that it is indeed $i\sigma_y$.

Alternative Nambu basis It is common for people to define instead the Nambu spinor in a rotated basis as such

$$\bar{\boldsymbol{c}}_i^\dagger = \begin{pmatrix} \boldsymbol{c}_i^\dagger & [i\sigma_y\boldsymbol{c}_i] \end{pmatrix} = \left(\begin{array}{cc|cc} c_{i\uparrow}^\dagger & c_{i\downarrow}^\dagger & c_{i\downarrow} & -c_{i\uparrow} \end{array}\right) \tag{52}$$

As also explained in section II.C.1 of the previous part, these basis' operators relate to each other as

$$\bar{\boldsymbol{c}}_i = \bar{\boldsymbol{\mathcal{U}}}\check{\boldsymbol{c}}_i \Leftrightarrow \check{\boldsymbol{c}}_i = \bar{\boldsymbol{\mathcal{U}}}^\dagger\bar{\boldsymbol{c}}_i \tag{53}$$

$$\bar{\boldsymbol{c}}_i^\dagger = \check{\boldsymbol{c}}_i^\dagger\bar{\boldsymbol{\mathcal{U}}}^\dagger \Leftrightarrow \check{\boldsymbol{c}}_i^\dagger = \bar{\boldsymbol{c}}_i^\dagger\bar{\boldsymbol{\mathcal{U}}} \tag{54}$$

and, consequently, for a generic $\check{\boldsymbol{M}}$ matrix,

$$\bar{\boldsymbol{M}} = \bar{\boldsymbol{\mathcal{U}}}\check{\boldsymbol{M}}\bar{\boldsymbol{\mathcal{U}}}^\dagger \tag{55}$$

with $\bar{\boldsymbol{\mathcal{U}}}$ is a unitary matrix (i.e $\bar{\boldsymbol{\mathcal{U}}}^{\dagger}\bar{\boldsymbol{\mathcal{U}}} = \bar{\boldsymbol{\mathcal{U}}}\bar{\boldsymbol{\mathcal{U}}}^{\dagger} = \mathbb{1}$)

$$\bar{\boldsymbol{\mathcal{U}}} = \begin{pmatrix} \sigma_0 & 0 \\ 0 & \imath\sigma_y \end{pmatrix} \tag{56}$$

Making use of Pauli matrices' property

$$\sigma_\alpha\sigma_\beta = \sigma = \sigma_0\delta_{\alpha\beta} + i\varepsilon_{\alpha\beta\gamma}\sigma_\gamma \tag{57}$$

one can check that

$$H_{\mathrm{K}} : \bar{\boldsymbol{\mathcal{U}}}[\tau_z \otimes \sigma_0]\bar{\boldsymbol{\mathcal{U}}}^{\dagger} = [\tau_z \otimes \sigma_0] \tag{58}$$

$$H_{\mathrm{SOC}} : \bar{\boldsymbol{\mathcal{U}}}[\tau_z \otimes \imath\sigma_y]\bar{\boldsymbol{\mathcal{U}}}^{\dagger} = [\tau_z \otimes \imath\sigma_y] \tag{59}$$

$$H_{\mathrm{Z}} : \bar{\boldsymbol{\mathcal{U}}}[\tau_z \otimes \sigma_z]\bar{\boldsymbol{\mathcal{U}}}^{\dagger} = [\tau_z \otimes \sigma_z] \tag{60}$$

$$H_{\mathrm{SC}} : \bar{\boldsymbol{\mathcal{U}}}[\tau_y \otimes \sigma_y]\bar{\boldsymbol{\mathcal{U}}}^{\dagger} = [\tau_x \otimes \sigma_0] \tag{61}$$

meaning that, in this the rotated basis, only the pairing Hamiltonian has it's Pauli matrices changed. Concretely,

$$H_{\mathrm{SC}} = \frac{1}{2}\Delta\sum_i \bar{\boldsymbol{c}}_i^{\dagger}[\tau_x \otimes \sigma_0]\bar{\boldsymbol{c}}_i \tag{62}$$

V. TOPOLOGICAL SUPERCONDUCTIVITY IN 2D MODELS

Need a intuitive and organized introduction relating all the nomenclatures "topological insulator", "Chern insulator" with the various effects. I still don't have a clear map of what's what and the subtle symmetry differences.

A. Quantum hall effect

B. Anomalous quantum Hall effect in the Haldane model

The quantum Hall effect without an external magnetic field is also referred to as the quantum anomalous Hall effect.

C. Quantum spin Hall effect in the Kane-Mele model

D. Integer quantum Hall effect

E. Fractional quantum Hall effect

VI. APPENDICES

A. Peierls substitution

The Peierls substitution method is a widely common approximation for describing tight-binding models in the presence of a slowly varying magnetic vector potential $\mathbf{A}(\mathbf{r})$. In a tight-binding scheme

it straightforwardly introduces a phase θ to hopping strength, dubbed the Peierls phase, such that the tight-binding hopping Hamiltonian reads instead

$$H_{\text{hop}} = t_{ij} e^{i\theta} c_j^\dagger c_i + h.c. \tag{63}$$

which directly follows from the gauge invariance of the time-dependent Schrodinger equation.

Proof: Consider the time-dependent Schrodinger equation describing such a system at the continuum limit, dubbed the Hofstadter Hamiltonian, reads

$$i\hbar \frac{\partial}{\partial t}\psi(\mathbf{r},t) = \left[\frac{i\hbar\boldsymbol{\nabla}_{\mathbf{r}} - \frac{e}{c}\mathbf{A}(\mathbf{r})}{2m} + eU(\mathbf{r},t)\right]\psi(\mathbf{r},t). \tag{64}$$

with $U(\mathbf{r})$ a generic scalar potential, for example the crystal lattice potential landscape. Furthermore, consider that one adds a local phase shift to the wavefunction as

$$\psi(\mathbf{r},t) \to e^{\frac{ie}{\hbar c}\Lambda(\mathbf{r},t)}\psi(\mathbf{r},t) \tag{65}$$

Substituting this ansatz directly into the time-dependent Schrödinger equation one obtains

$$e^{\frac{ie}{\hbar c}\Lambda}\left(i\hbar\frac{\partial}{\partial t} - \frac{e}{c}\frac{\partial\Lambda}{\partial t}\right)\psi = e^{\frac{ie}{\hbar c}}\frac{1}{2m}\left(-i\hbar\boldsymbol{\nabla} - \frac{e}{c}\mathbf{A} + \frac{e}{c}\boldsymbol{\nabla}\Lambda + 2meU\right)^2\psi$$

where we have omitted the spacial and temporal dependency for simplicity. See that if one now defines the potentials as

$$\mathbf{A} \to \mathbf{A} + \boldsymbol{\nabla}\Lambda$$
$$U \to U + \frac{1}{c}\frac{\partial\Lambda}{\partial t}$$

one recovers the original equation. This means that applying the gauge transformation (meaning that there exists other physical descriptions of the system that leaves the free energy unchanged) to $\mathbf{A}$ and U is equivalent to multiplying the state by a phase factor, albeit one that changes in space and time.

B. Overview of simpler systems

1. *Linear lattice*

2. *Square lattice*

C. Overview of graphene systems

1. *Monolayer graphene*

Hexagonal boron nitride (hBN) is a 2D material composed of a simple layer of alternating boron and nitrogen atoms disposed in a planar honeycomb lattice, as shown in Fig.(13)(a). The Bravais lattice

$$\mathbf{r}_i = n_{i1}\mathbf{a}_1 + n_{i2}\mathbf{a}_2, \quad n_{i1}, n_{i2} \in \mathbb{Z} \tag{66}$$

is generated by the real vectors basis

$$\mathbf{a}_1 = a_0\begin{bmatrix}+\sin(30^\circ)\\ +\cos(30^\circ)\end{bmatrix} \text{ and } \mathbf{a}_2 = a_0\begin{bmatrix}+\sin(30^\circ)\\ -\cos(30^\circ)\end{bmatrix}. \tag{67}$$

where $\sin(30°) = 1/2$ and $\cos(30°) = \sqrt{3}/2$. In each diamond shaped Wigner-Seitz primitive cell (depicted in yellow), we have one boron atom and one nitride atom, which we designate as sub-lattices A (depicted in red) and B (depicted in blue) respectively. The atoms within the central primitive cell are located at

$$\mathbf{s}_A = \frac{a_0}{\sqrt{3}} \begin{bmatrix} 0 \\ -1/2 \end{bmatrix} \text{ and } \mathbf{s}_B = \frac{a_0}{\sqrt{3}} \begin{bmatrix} 0 \\ +1/2 \end{bmatrix}. \tag{68}$$

where the origin is defined at the midpoint between the atoms. For each site A, the position of the nearest-neighbors (NN) in the sites B are given by

$$\boldsymbol{\delta}_1 = \frac{a_0}{\sqrt{3}} \begin{bmatrix} 0 \\ 1 \end{bmatrix}, \boldsymbol{\delta}_2 = \frac{a_0}{\sqrt{3}} \begin{bmatrix} +\sin(60°) \\ -\cos(60°) \end{bmatrix} \text{ and } \boldsymbol{\delta}_3 = \frac{a_0}{\sqrt{3}} \begin{bmatrix} -\sin(60°) \\ -\cos(60°) \end{bmatrix}. \tag{69}$$

where $\sin(60°) = \sqrt{3}/2$ and $\cos(60°) = 1/2$. All these vectors are shown in Fig.(13)(a) within the real space lattice. Furthermore, from the real lattice basis vectors, in order to fulfill $\boldsymbol{a}_i \cdot \boldsymbol{b}_j = 2\pi\delta_{ij}$, the reciprocal lattice basis vectors follow as

$$\mathbf{b}_1 = \frac{2\pi}{a_0} \begin{bmatrix} +\cos(30°) \\ -\sin(30°) \end{bmatrix} \text{ and } \mathbf{b}_2 = \frac{2\pi}{a_0} \begin{bmatrix} +\cos(30°) \\ +\sin(30°) \end{bmatrix}. \tag{70}$$

These are also shown in Fig.(13)(b) together with the first zone of Brillouin, formed by the area enclosed by the intersection of their bisectrices. The high-simmetry points are Γ, the origin, the Dirac points $K_\pm$ and M read as

$$\boldsymbol{\Gamma} = \begin{bmatrix} 0 \\ 0 \end{bmatrix}, \quad K_\pm = \pm\frac{4\pi}{3a_0} \begin{bmatrix} 1 \\ 0 \end{bmatrix} \text{ and } M = \frac{2\pi}{a_0} \begin{bmatrix} +\cos(30°)/2 \\ +\sin(30°)/2 \end{bmatrix} \tag{71}$$

where the K point is found such that $\left(\mathbf{M} + K_{k_x}\hat{\mathbf{M}}_\perp\right)_{k_y} = 0$, with $\hat{\mathbf{M}}_\perp$ the unit vector in the perpendicular direction to $\mathbf{M}$. In far right side of Fig.(12), we make a note that the discretized grid it's in the Bloch momentums basis $\{\phi_1, \phi_2\}$, i.e in the direction of the reciprocal lattice vectors, and not simply in the reciprocal space $\{k_x, k_y\}$. In the Bloch momentums basis the Dirac points would reads as $K_\pm = 2\pi/3a_0 \left[\pm 1, \ \mp 1\right]$.

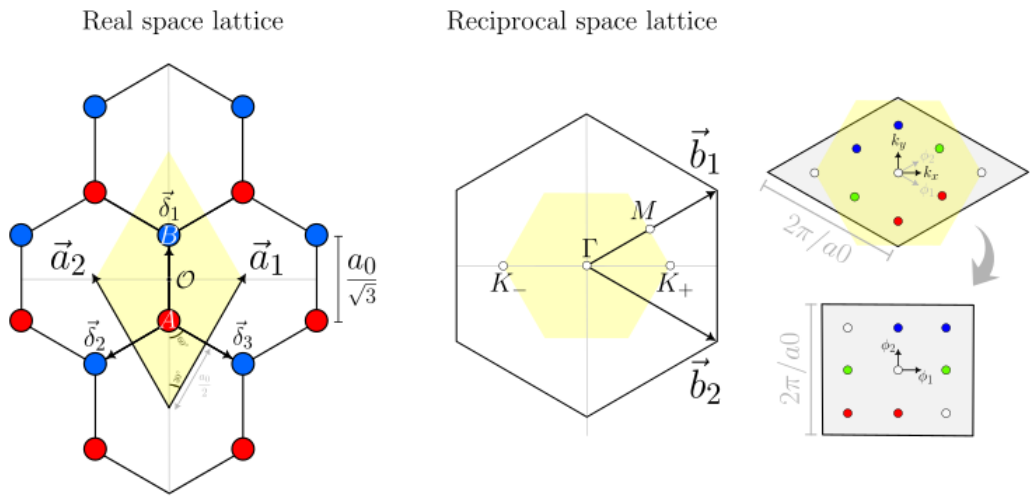

Figure 12.

Let us consider the nearest-neighbors (NN) tight-binding model, written in real space as

$$H_{\mathrm{TB}}(\mathbf{R}) = \sum_i \epsilon_A a^\dagger_{\mathbf{r}_i} a_{\mathbf{r}_i} + \sum_i \epsilon_B b^\dagger_{\mathbf{r}_i} b_{\mathbf{r}_i} - t \sum_{\langle i,j \rangle} \left(a^\dagger_{\mathbf{r}_i} b_{\mathbf{r}_i + \boldsymbol{\delta}_j} + b^\dagger_{\mathbf{r}_j} a_{\mathbf{r}_i - \boldsymbol{\delta}_j} \right), \tag{72}$$

where the operators $a^\dagger_{\mathbf{r}_i}(a_{\mathbf{r}_i})$ create (annihilate) an electron in the sub-lattice A in a given Bravais lattice site $\mathbf{r}_i$, the operators $b^\dagger_{\mathbf{r}_i}(b_{\mathbf{r}_i})$ the same but for sub-lattice B, ϵ_A and ϵ_B are the onsite energies of site A and B respectively, and t is the hopping strength between nearest-neighbouring sites A and B and back, denoted with $\langle i,j \rangle$.

Expressing the creation/annihilation operators as their Fourier counterparts,

$$a_{\mathbf{R}_i} = \frac{1}{\sqrt{V}} \sum_{\mathbf{k}} e^{+i\mathbf{k}\cdot(\mathbf{R}_i + \mathbf{s}_A)} a_{\mathbf{k}} \quad \text{and} \quad b_{\mathbf{R}_i} = \frac{1}{\sqrt{V}} \sum_{\mathbf{k}} e^{+i\mathbf{k}\cdot(\mathbf{R}_i + \mathbf{s}_B)} b_{\mathbf{k}}, \tag{73}$$

and using the identity $\delta(\mathbf{k} - \mathbf{k}') = 1/N \sum_i e^{-i\mathbf{R}_i \cdot (\mathbf{k} - \mathbf{k}')}$, we obtain the Hamiltonian in reciprocal space,

$$H_{\mathrm{TB}}(\mathbf{R}) = \sum_{\mathbf{k}} \epsilon_A a^\dagger_{\mathbf{k}} a_{\mathbf{k}} + \sum_{\mathbf{k}} \epsilon_B b^\dagger_{\mathbf{k}} b_{\mathbf{k}} - t \sum_{\mathbf{k}} \left(\gamma_{\mathbf{k}} a^\dagger_{\mathbf{k}} b_{\mathbf{k}} + \gamma^\dagger_{\mathbf{k}} b^\dagger_{\mathbf{k}} a_{\mathbf{k}} \right), \tag{74}$$

where $\gamma_{\mathbf{k}} = \sum_{\langle j \rangle} \exp(+i\mathbf{k} \cdot \boldsymbol{\delta}_j)$ is complex number. If we now define a row vector $c^\dagger_{\mathbf{k}} = \begin{bmatrix} a^\dagger_{\mathbf{k}} & b^\dagger_{\mathbf{k}} \end{bmatrix}$ we can rewrite the system's Hamiltonian as $H^{\mathrm{TB}}_{\mathbf{R}} = \sum_{\mathbf{k}} c^\dagger_{\mathbf{k}} H^{\mathrm{TB}}_{\mathbf{k}} c_{\mathbf{k}}$ with

$$H_{\mathrm{TB}}(\mathbf{k}) = \begin{bmatrix} \epsilon_A & -t\gamma_{\mathbf{k}} \\ -t\gamma^\dagger_{\mathbf{k}} & \epsilon_B \end{bmatrix}. \tag{75}$$

Within this simplified tight-binding model, the expression for the electronic two-band structure can easily be obtained analytically by diagonalizing the matrix in Eq.(75), yielding

$$E^{\pm}_{\mathrm{TB}}(\mathbf{k}) = \pm \sqrt{\epsilon^2 + t^2 \left[3 + 2\cos(a_0 k_x) + 4\cos\left(\frac{a_0\sqrt{3}}{2} k_y \right) \cos\left(\frac{a_0}{2} k_x \right) \right]}, \tag{76}$$

having defined the zero point energy at $(\epsilon_A + \epsilon_B)/2$ and defined $\epsilon \equiv (\epsilon_A - \epsilon_B)/2$ at the middle of the gap such that $\epsilon_A = \epsilon$ and $\epsilon_B = -\epsilon$. The valence band corresponds to the $E^-_{\rm TB}(\mathbf{k})$ dispersion while the $E^+_{\rm TB}(\mathbf{k})$ corresponds to the conduction band, as shown in Fig.(13)(c). The band structure is accompanied by the density of states $\mathrm{DoS}(E) = \sum_{\mathbf{k}} \delta\left(E - E(\mathbf{k})\right)$.

Notice that, if $\epsilon_A = \epsilon_B$, as is the case for graphene, we obtain $\epsilon = 0$ and the band dispersion closes in a linear fashion at the so called Dirac points. In hBN, the electronic band dispersion is also at its minimum near these points but has instead a parabolic shape. In either case, this points represent a fundamental symmetry of the system, called valley parity. To see why the dispersion is parabolic at these valley points, we Taylor series expand the exponential of $\gamma_{\mathbf{k}}$ in Eq.(**??**) near $\mathbf{k} \to \mathbf{K} + \mathbf{p}$ with $\mathbf{p} \to 0$. We obtain $\exp(+i\mathbf{p}\cdot\boldsymbol{\delta}_j) \approx 1 + i\mathbf{p}\cdot\boldsymbol{\delta}_j$. Now, since $\sum_{\langle j\rangle} \exp(+i\mathbf{K}\cdot\boldsymbol{\delta}_j) = 0$ we are left with $\gamma_{\mathbf{K}+\mathbf{p}} \simeq i\mathbf{p}\cdot\sum_{\langle j\rangle} \exp(+i\mathbf{K}\cdot\boldsymbol{\delta}_j)\boldsymbol{\delta}_j = -\sqrt{3}a_0/2\,(p_x - ip_y)$. Invoking the Pauli matrices definitions, from Eq.(75) we can write the TB Hamiltonian $H^{\mathbf{k}}_{\rm TB}$ in this low-energy regime as

$$H_{\rm TB}(\mathbf{K}+\mathbf{p}) = \epsilon\sigma_z + t\frac{\sqrt{3}a_0}{2}\left(\mathbf{p}\cdot\boldsymbol{\sigma}\right), \tag{77}$$

which clearly resembles the 2D Dirac Hamiltonian, $H_{\rm Dirac} = \sigma_z mc^2 + c\left(\mathbf{p}\cdot\boldsymbol{\sigma}\right)$ with ϵ taking the role of the rest mass energy mc^2 and instead with a velocity $v_F = t\sqrt{3}a_0/2$, termed the *Fermi velocity*, as a replacement to the velocity of light c. Notice that, for the case of graphene, since $\epsilon = 0$, the electrons would behave as if they are massless. In this limit, the hBN low-energy dispersion can be written as the typical relativistic dispersion relation

$$E_{\rm TB}(\mathbf{K}+\mathbf{p}) = \pm\sqrt{p^2v_F^2 + m_{\rm eff}^2 v_F^4}. \tag{78}$$

where $m_{\rm eff}$ is the effective mass of the electron at a given point near the valleys.

Refazer esta figura em Quantica para aprender a fazer densidade de estados. Falar das singularidades de van Hove.

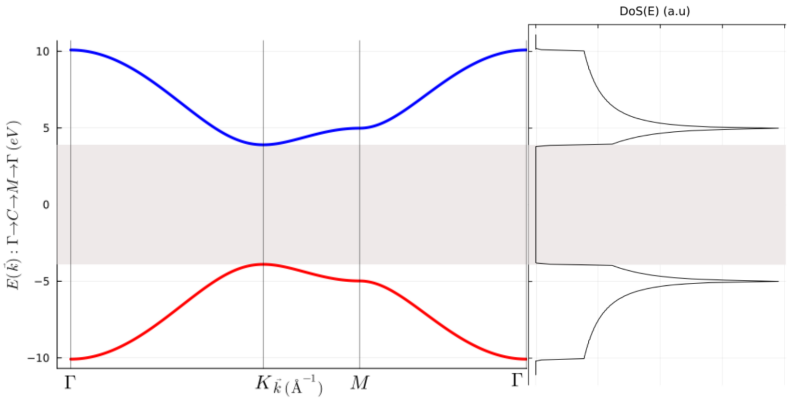

Figure 13. hBN electronic band structure from a nearest-neighbor tight-binding model accompanied by the density of the states. The dispersion goes along the symmetry path $\mathbf{k} : \Gamma \to K \to M \to \Gamma$ and was calculated using $\epsilon_g = 7.8$eV for the energy gap, $t = 3.1$eV for the hopping parameter and $a_0 = 1.42\sqrt{3}$Å for the honeycomb lattice length.

2. *Bilayer Bernal graphene*

Consider a bilayer graphene model depicted in Fig.(14).

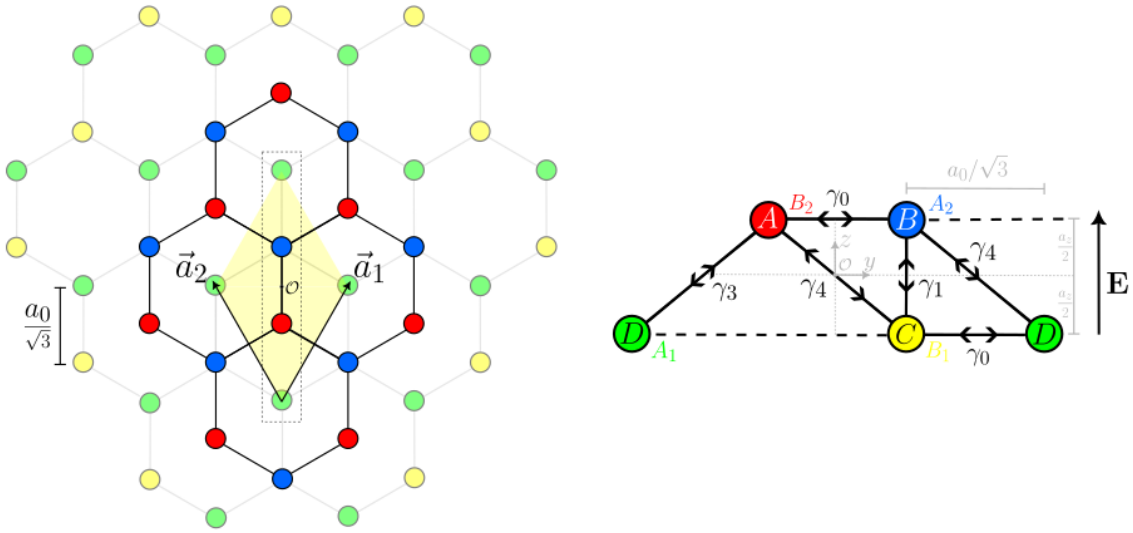

Figure 14. **(a)** Top view of the bilayer graphene **(b)** Side view of the dotted region in (a)

The tight-binding Hamiltonian of such a model reads

$$
\begin{aligned}
H_{\mathrm{BLG}} &= H_{\mathrm{intralayer}} + H_{\mathrm{interlayer}} = (H_{\mathrm{top}} + H_{\mathrm{bot}}) + (H_{\gamma_1} + H_{\gamma_3} + H_{\gamma_4}) \\
H_{\mathrm{top}} &= \sum_i (\epsilon_A - \mu)\, c_i^\dagger a_i + \sum_i (\epsilon_B - \mu)\, b_i^\dagger b_i - \gamma_0 \sum_{\langle i,j \rangle} \left(a_i^\dagger b_j + h.c \right) \\
H_{\mathrm{bot}} &= \sum_i (\epsilon_C - \mu)\, c_i^\dagger c_i + \sum_i (\epsilon_D - \mu)\, d_i^\dagger d_i - \gamma_0 \sum_{\langle i,j \rangle} \left(c_i^\dagger d_j + h.c \right) \\
H_{\gamma_1} &= +\gamma_1 \sum_{\langle i,j \rangle} \left(b_i^\dagger c_j + h.c \right) \\
H_{\gamma_3} &= -\gamma_3 \sum_{\langle i,j \rangle} \left(a_i^\dagger d_j + h.c \right) \\
H_{\gamma_4} &= +\gamma_4 \sum_{\langle i,j \rangle} \left(b_i^\dagger d_j + h.c \right) + t_4 \sum_{\langle i,j \rangle} \left(a_i^\dagger C_j + h.c \right)
\end{aligned}
$$

Here, a site located at $\mathbf{r}_i$ is indexed by the side index i and its next nearest neighbors located at $\mathbf{r}_j$ are indexed with the site index j. Of course, $\mathbf{r}_j$ depends on the kind of hopping in questions: for γ_0 it's $\mathbf{r}_j = \mathbf{r}_i + \boldsymbol{\delta}_j$ with $j = 1, 2, 3$, for γ_1 it's $\mathbf{r}_j = \mathbf{r}_i \pm a_z \hat{\mathbf{z}}$, and for γ_3 and γ_4 it's $\mathbf{r}_j = \mathbf{r}_i + \boldsymbol{\delta}_j \pm a_z \hat{\mathbf{z}}$. Moreover, let us consider an electric field $\mathbf{E}$ uniform in the plane $x\mathcal{O}y$ and growing along the $\hat{\mathbf{z}}$, described by the tight-binding Hamiltonian

$$
H_E = \sum_i E_i \left(f_{i\uparrow}^\dagger f_{i\uparrow} - f_{i\downarrow}^\dagger f_{i\downarrow} \right)
$$

where $E_i = E \times z_i$ is the amplitude of the electric field at position $\mathbf{r}_i$, only really dependent on z_i, and $f_i^\dagger = \begin{bmatrix} f_{i\uparrow}^\dagger & f_{i\downarrow}^\dagger \end{bmatrix}$ is a generic fermionic operator. Since in our bilayer model the bottom layer is situated at $z = 0$ we redefine $E(a_z) = E$, such that

$$
H_{\mathrm{BLG}} + = E \sum_i \left\{ \left(a_{i\uparrow}^\dagger a_{i\uparrow} - a_{i\downarrow}^\dagger a_{i\downarrow} \right) + \left(b_{i\uparrow}^\dagger b_{i\uparrow} - b_{i\downarrow}^\dagger b_{i\downarrow} \right) \right\}
$$

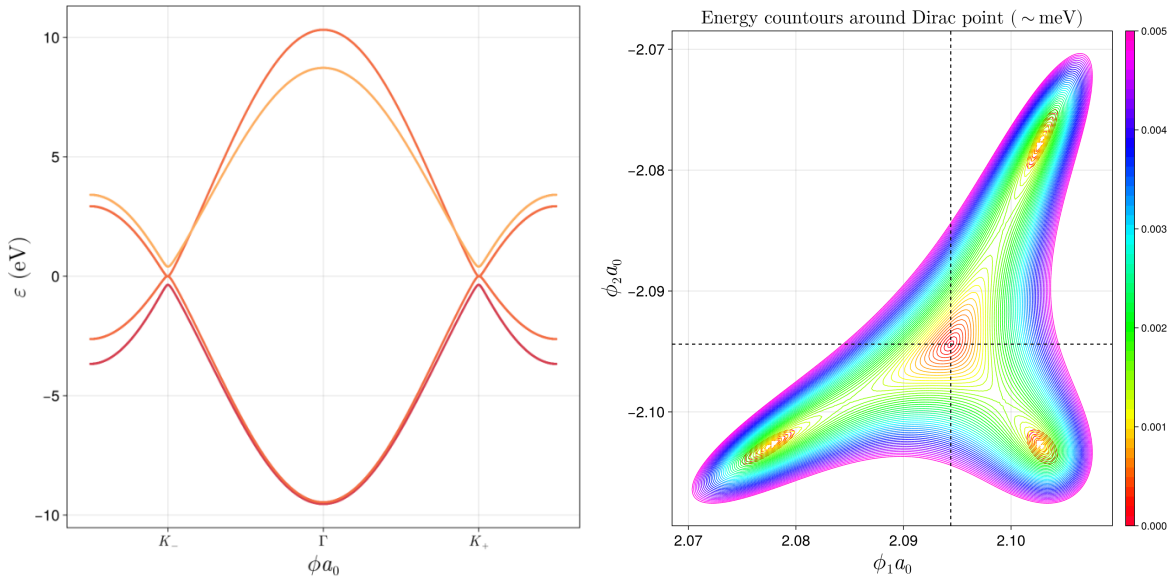

Figure 15. **(a, b)** Bandstructure along symmetry path $\Gamma \to K_+ \to M$ and **(c)** trigonal warping of BLG around the Dirac point K_+.

Armchair and Zigzag configurations

3. Twisted bilayer graphene

4. Kekulé modulation

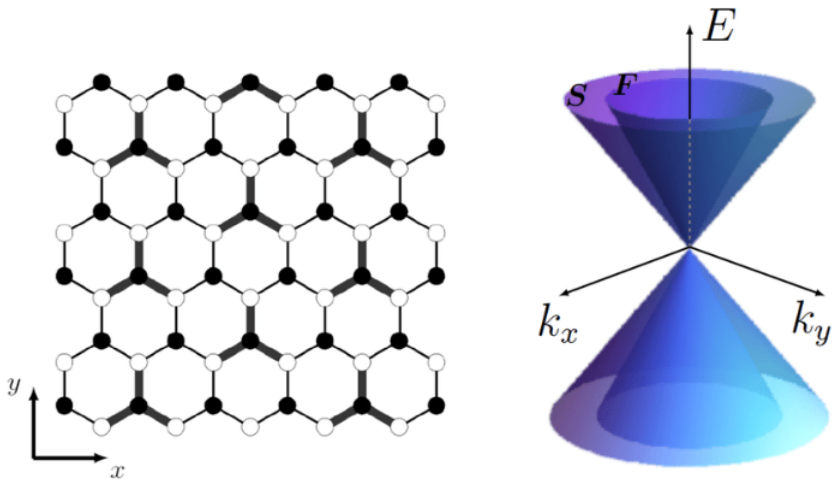

Figure 16. Caption

BIBLIOGRAPHY

As you been noticing, there is no references whatsoever within the text. Because these are personal journal notes, I preferred to avoid the hassle of managing minor references altogether, since, to be honest, one just skims through those (at best). I will, however, cite the actually relevant chapters/sections of papers/notes/courses/book that I closely followed for the making of this notes.

For Part I "Introduction to superconductivity theory" I mostly followed **Tinkham's "Introduction to superconductivity"** at [Dover publisher link] and **Rashid's "Lecture notes: Superconductivity"** at [personal website link] for both chapter structure and content. For Part II "Introduction to topological superconductivity" I closely followed **Akhmerov's "Online course on topology in condensed matter"** at https://topocondmat.org/ and **Asboth's "A short course on topological insulators"** at arXiv:1509.02295.. for both chapter structure and content. Moreover for "Concepts of symmetry and topology" and the "SSH chain model" I additionally refer to **Tiago Antão's Master thesis on "Disorder and Topology in Spin Systems"** at [uni repositorium link] For the "Kitaev model" and "Oreg-Lutchyn model" I refer, respectively, to the original papers of **Kitaev's "Unpaired Majorana fermions in quantum wires"** at Phys.-Usp. 44 131, and **Lutchyn's "Majorana Fermions and a Topological Phase Transition in Semiconductor-Superconductor Heterostructures"** at Phys. Rev. Lett. 105, 077001 and **Oreg's "Helical liquids and Majorana bound states in quantum wires"** at Phys. Rev. Lett. 105, 177002.